Omnidirectional Camera Model and Epipolar Geometry Estimation by RANSAC with bucketing

Branislav Mičušík and Tomáš Pajdla

Center for Machine Perception
http://cmp.felk.cvut.cz
Department of Cybernetics
Faculty of Electrical Engeneering
Czech Technical University in Prague

Motivation

- Multiple view geometry of standard perspective cameras using point correspondences

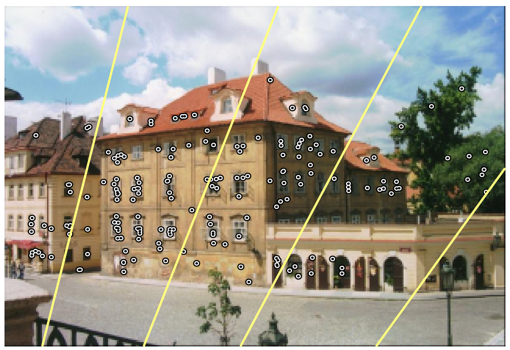

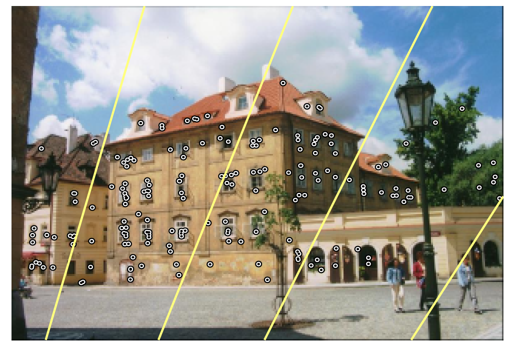

Motivation

- Multiple view geometry of standard perspective cameras using point correspondences

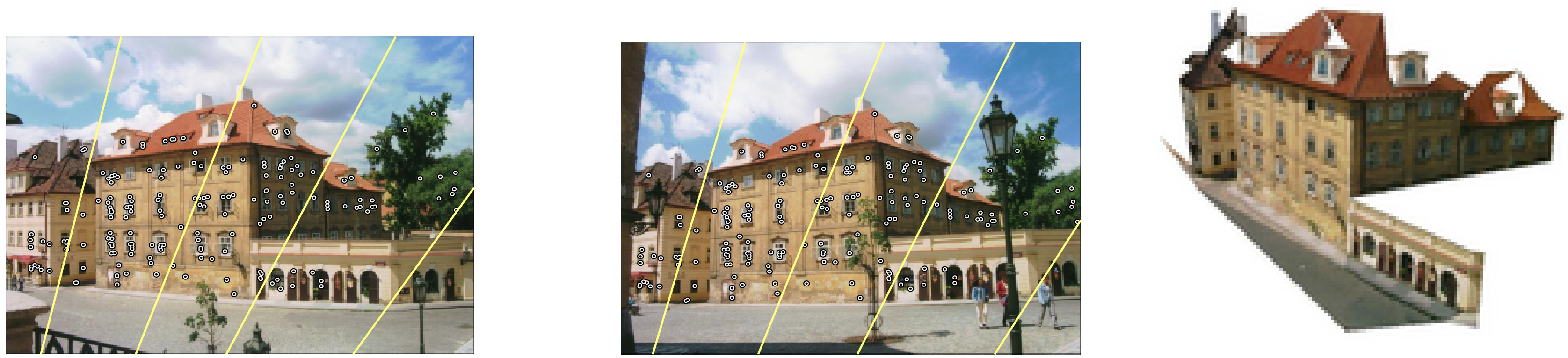

- Multiple view geometry of uncalibrated omnidirectional non-perspective cameras using point correspondences

Contribution & Outline

Our Contribution:

- Epipolar geometry estimation and omnidirectional camera calibration by RANSAC with bucketing for very wide ($> 180°$) view angle

- Generalization of

  A. Fitzgibbon: Simultaneous linear estimation of multiple view geometry and lens distortion. *CVPR*, 2001.

  to an omnidirectional cameras

Contribution & Outline

Our Contribution:

- Epipolar geometry estimation and omnidirectional camera calibration by RANSAC with bucketing for very wide ($> 180°$) view angle

- Generalization of

  A. Fitzgibbon: Simultaneous linear estimation of multiple view geometry and lens distortion. *CVPR*, 2001.

  to an omnidirectional cameras

Outline:

- Omnidirectional image formation
- Omnidirectional camera calibration via an epipolar geometry estimation
- Problems with nonlinear camera model fitting
- Robust method based on RANSAC with bucketing

Omnidirectional cameras possessing central projection

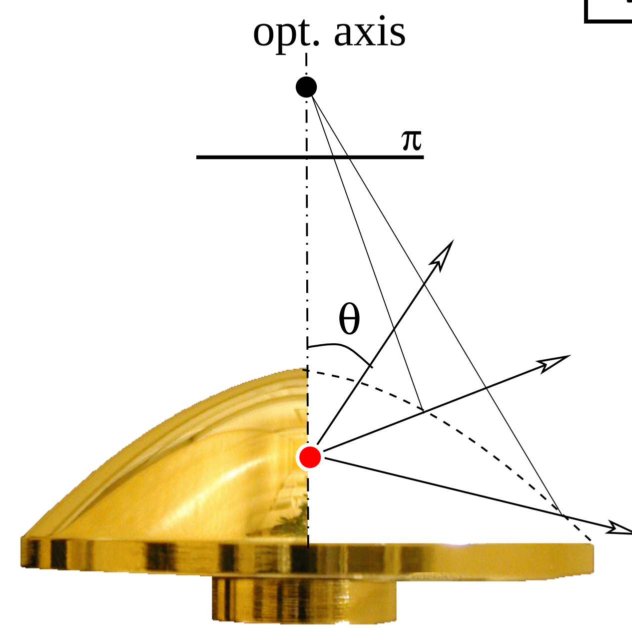

Omnidirectional catadioptric camera

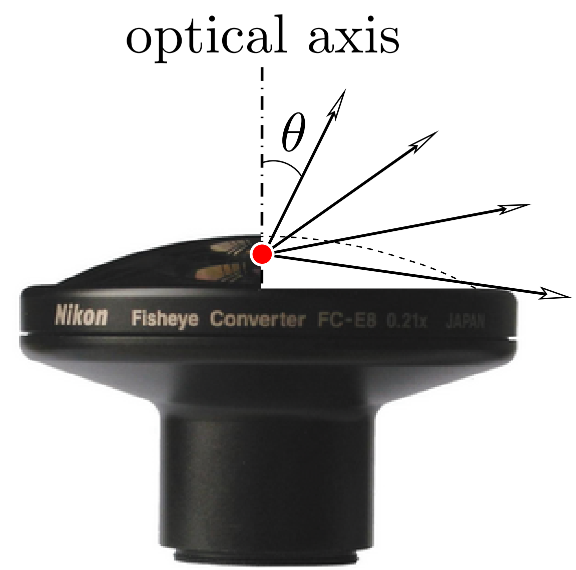

Fisheye lens with angle of view above 180°

Epipolar geometry

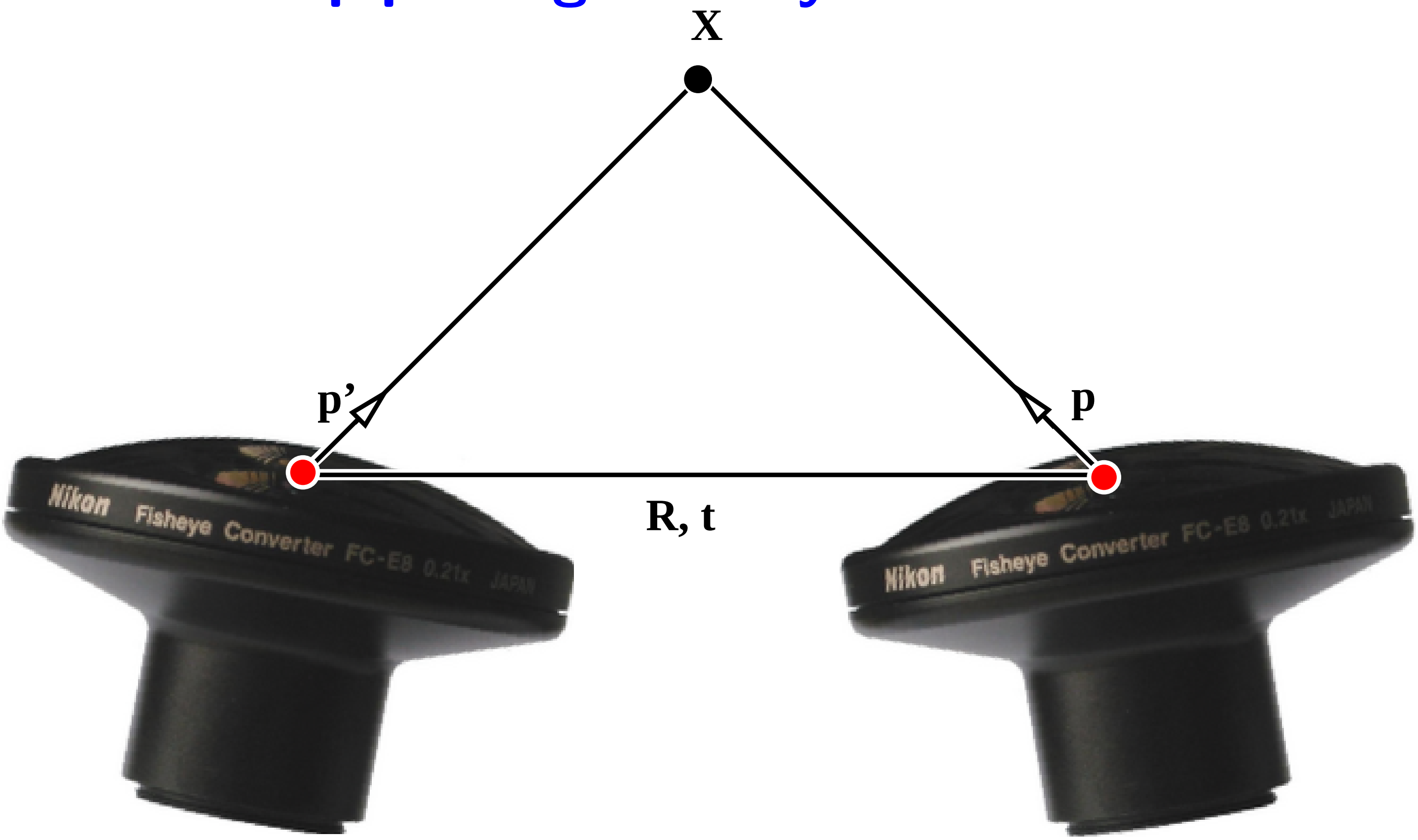

- central omnidirectional cameras posses an epipolar geometry

Epipolar geometry

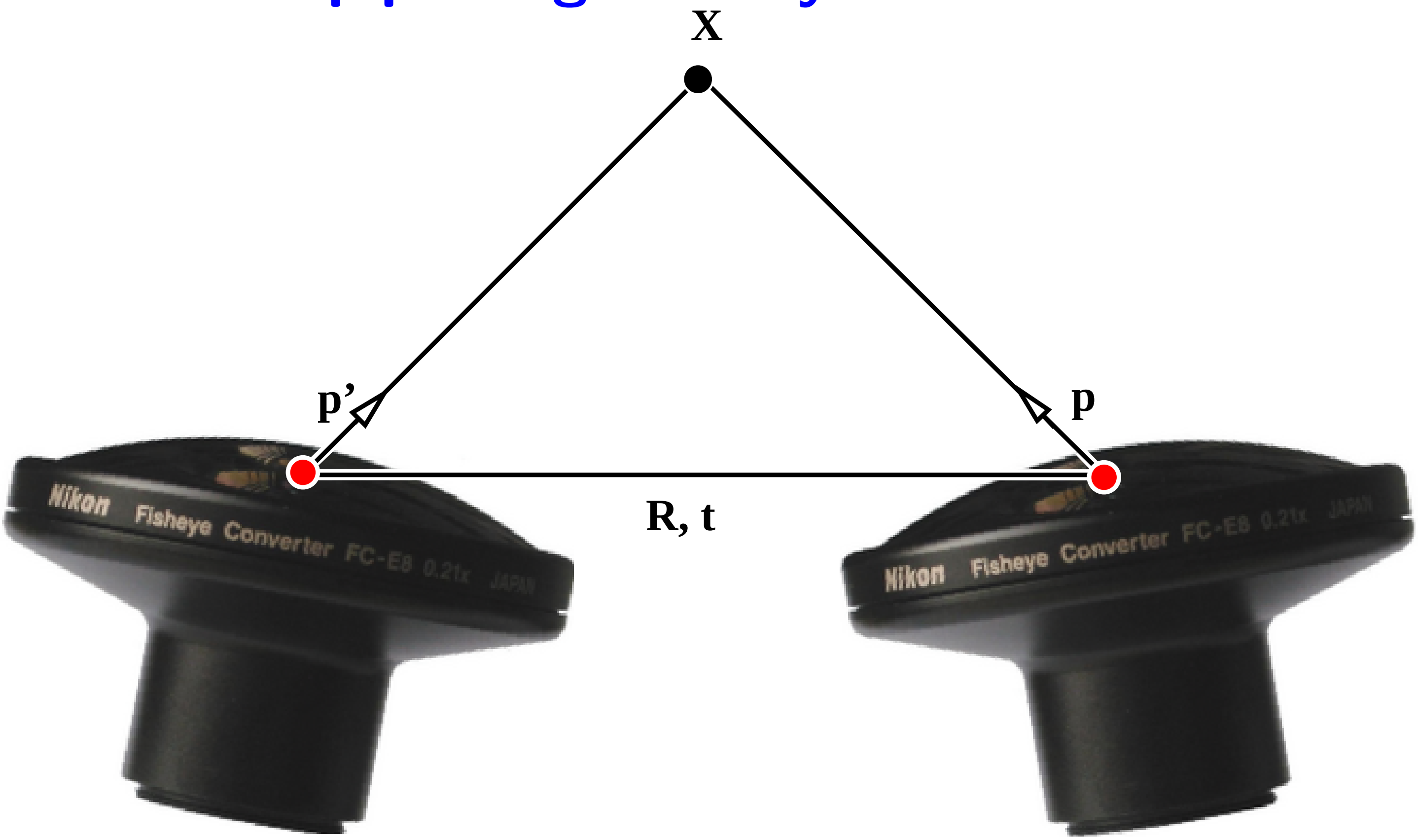

- central omnidirectional cameras posses an epipolar geometry

$$\mathbf{p'}^\top \mathbf{F}\mathbf{p} = 0$$

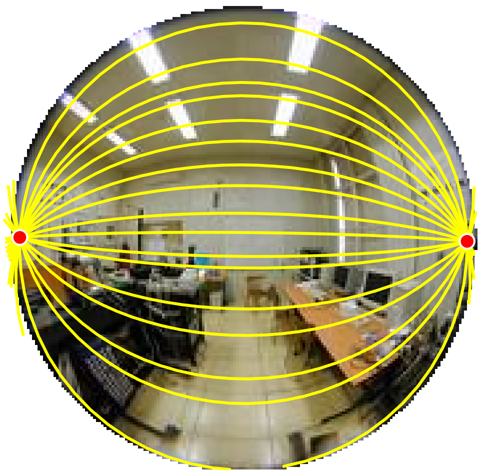

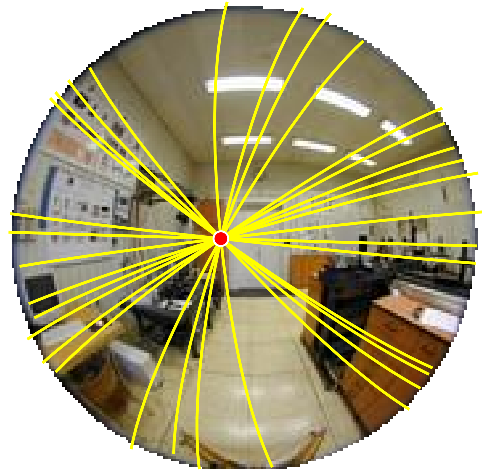

Omnidirectional camera calibration

- B.Mičušík and T.Pajdla: Estimation of omnidirectional camera model from epipolar geometry. *CVPR*, 2003, Madison

Omnidirectional camera calibration

- B.Mičušík and T.Pajdla: Estimation of omnidirectional camera model from epipolar geometry. $CVPR$, 2003, Madison
- Precalibration step

Omnidirectional camera calibration

- B.Mičušík and T.Pajdla: Estimation of omnidirectional camera model from epipolar geometry. *CVPR*, 2003, Madison
- Precalibration step

Omnidirectional camera calibration

- B.Mičušík and T.Pajdla: Estimation of omnidirectional camera model from epipolar geometry. $CVPR$, 2003, Madison
- Precalibration step

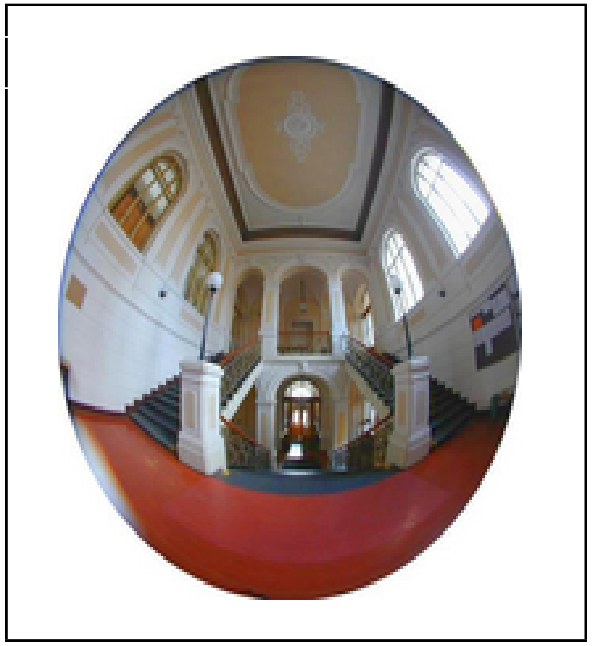

Omnidirectional camera calibration

- B.Mičušík and T.Pajdla: Estimation of omnidirectional camera model from epipolar geometry. *CVPR*, 2003, Madison
- Precalibration step

Omnidirectional camera calibration

- B.Mičušík and T.Pajdla: Estimation of omnidirectional camera model from epipolar geometry. *CVPR*, 2003, Madison
- Precalibration step

Omnidirectional camera calibration

- B.Mičušík and T.Pajdla: Estimation of omnidirectional camera model from epipolar geometry. $CVPR$, 2003, Madison
- Precalibration step

After precalibration step

- an image of an optical axis, square pixels and skew parameter are obtained

Omnidirectional camera calibration

- B.Mičušík and T.Pajdla: Estimation of omnidirectional camera model from epipolar geometry. *CVPR*, 2003, Madison
- Precalibration step

After precalibration step

- an image of an optical axis, square pixels and skew parameter are obtained
- a non-linear mapping becomes radially symmetric

From image point to 3D ray

From image point to 3D ray

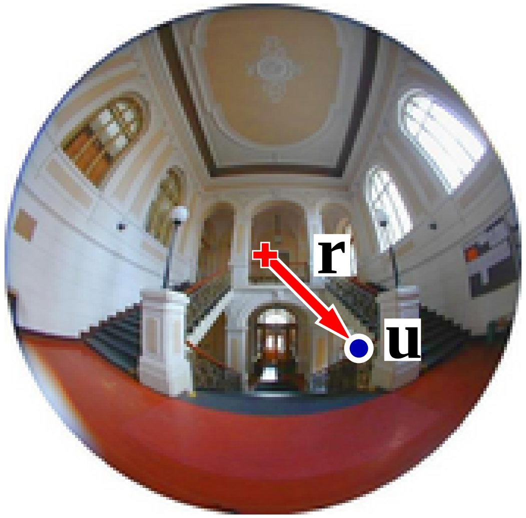

From image point to 3D ray

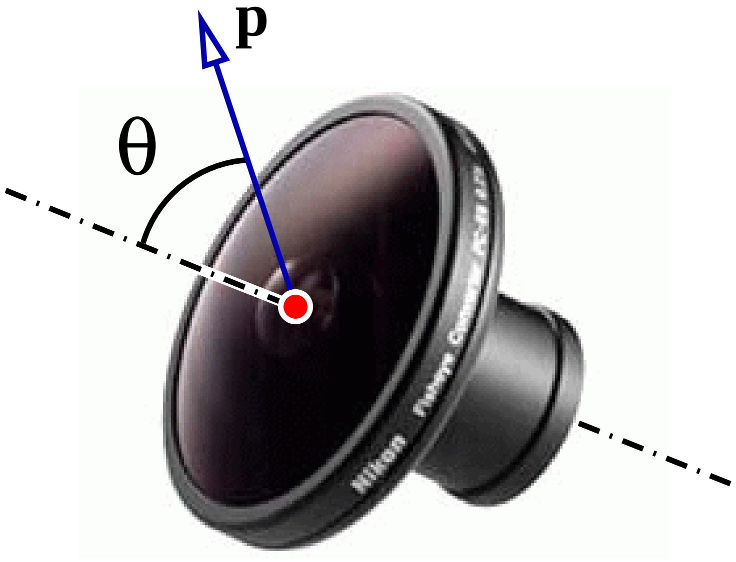

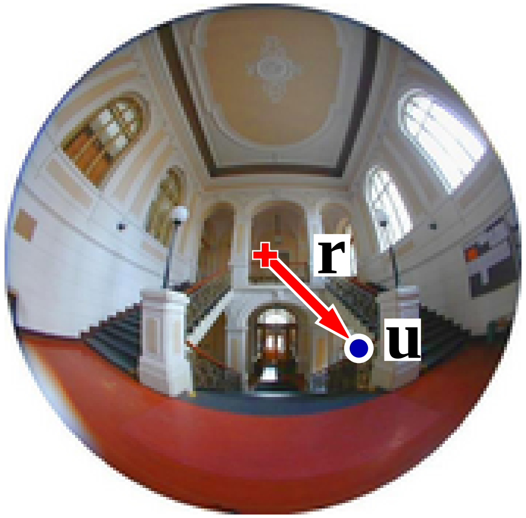

From image point to 3D ray

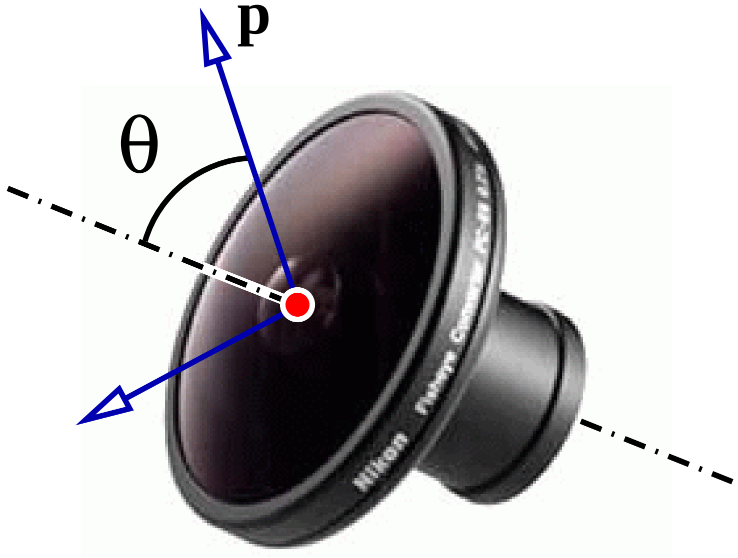

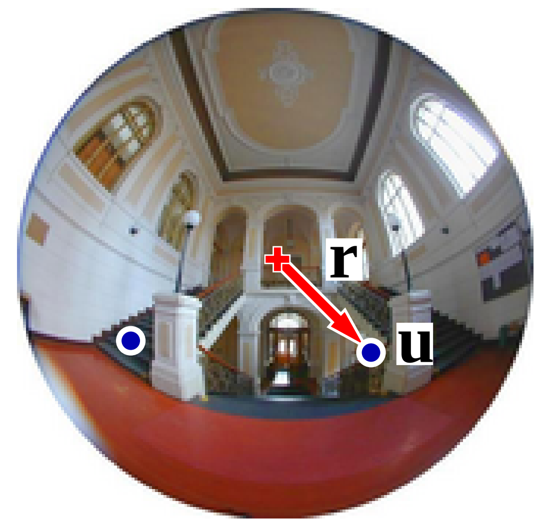

From image point to 3D ray

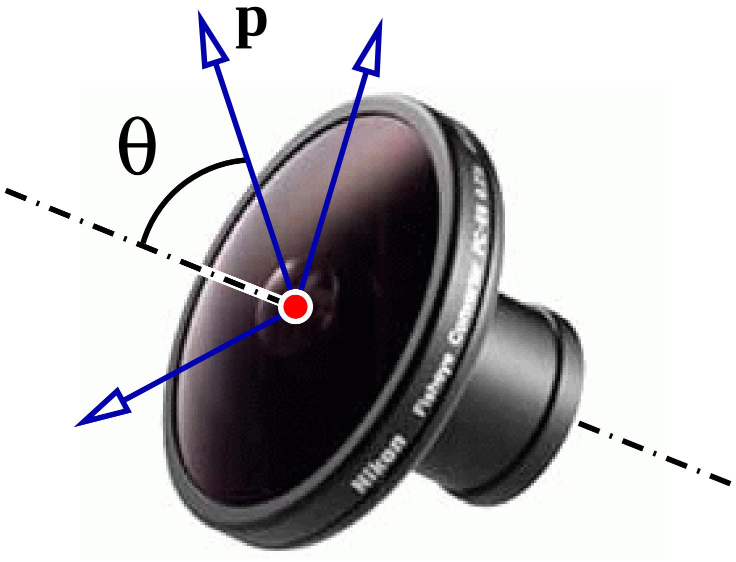

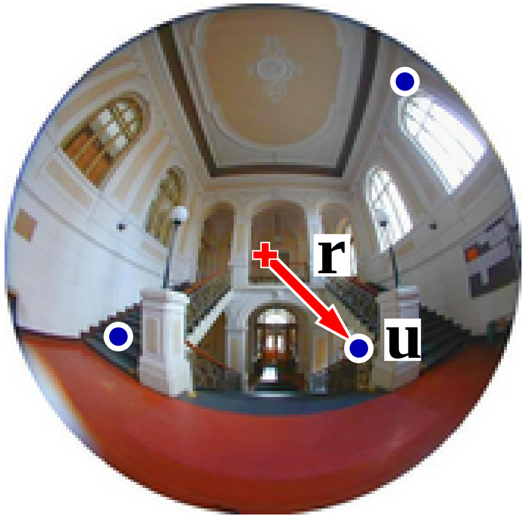

From image point to 3D ray

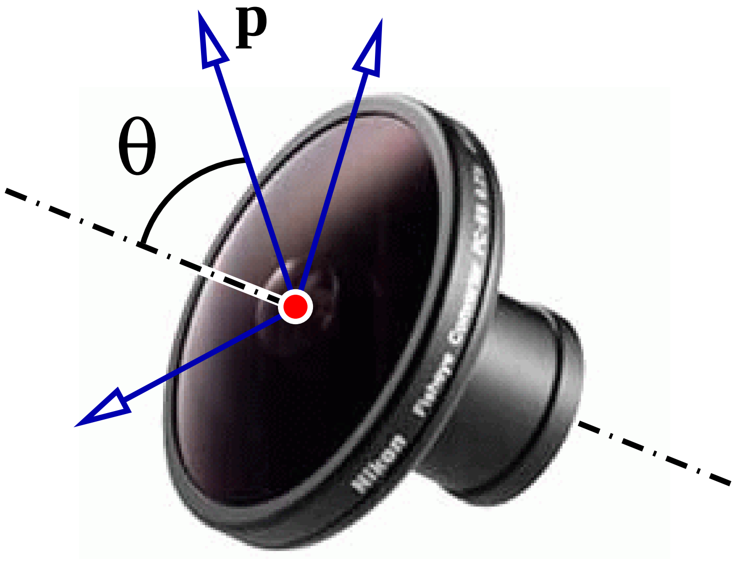

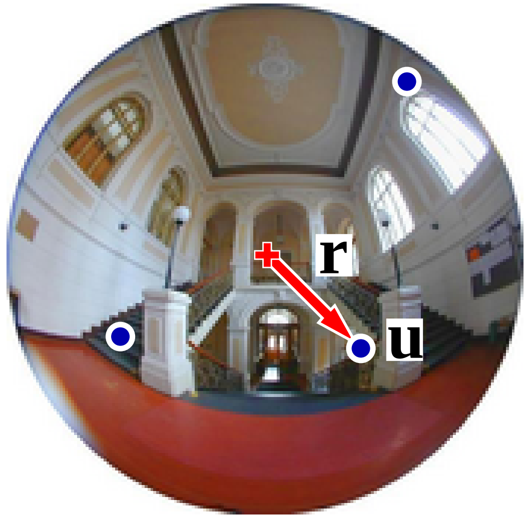

- Relation between 3D vectors and image points is captured by a non-linear function, e.g.

$$\theta = \frac{ar}{1+br^2}$$

From image point to 3D ray

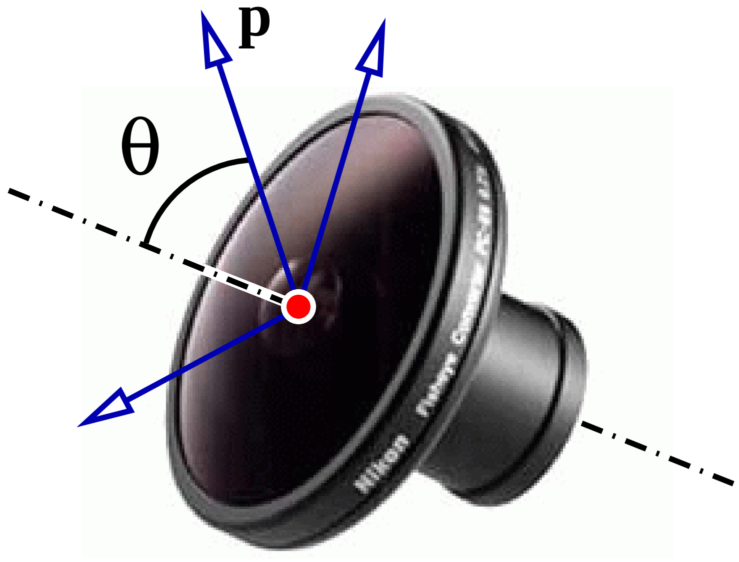

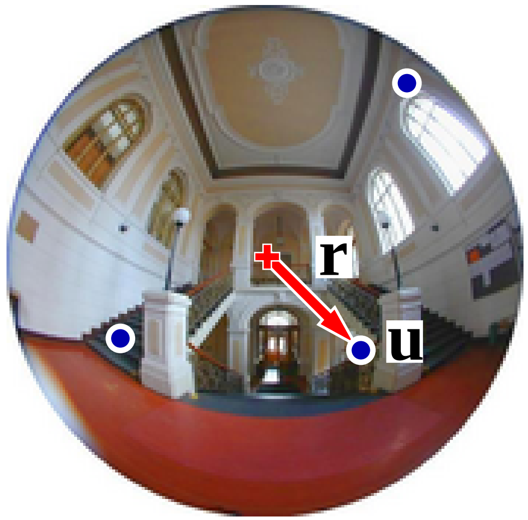

- Relation between 3D vectors and image points is captured by a non-linear function, e.g.

$$\theta = \frac{ar}{1+br^2}$$

- 3D vector corresponding to an image point:

$$\mathbf{p} \simeq g(\mathbf{u}) = \begin{pmatrix} \mathbf{u} \\ w \end{pmatrix} = \begin{pmatrix} \mathbf{u} \\ f(\mathbf{u}, a, b) \end{pmatrix} = \begin{pmatrix} \mathbf{u} \\ \frac{r}{\tan\theta} \end{pmatrix} = \begin{pmatrix} \mathbf{u} \\ \frac{r}{\tan\frac{ar}{1+br^2}} \end{pmatrix}$$

details 1 2

Theory of omnidirectional camera calibration

- Taylor series of g with respect to parameters a, b

$$\mathbf{p} \quad \simeq \quad g(\mathbf{u}) = \begin{pmatrix} \mathbf{u} \\ \frac{r}{\tan \frac{ar}{1+br^2}} \end{pmatrix} \approx \mathbf{x} + a\mathbf{s} + b\mathbf{t}$$

Theory of omnidirectional camera calibration

- Taylor series of g with respect to parameters a, b

$$\mathbf{p} \simeq g(\mathbf{u}) = \begin{pmatrix} \mathbf{u} \\ \frac{r}{\tan \frac{ar}{1+br^2}} \end{pmatrix} \approx \mathbf{x} + a\mathbf{s} + b\mathbf{t}$$

- Epipolar constraint for rays

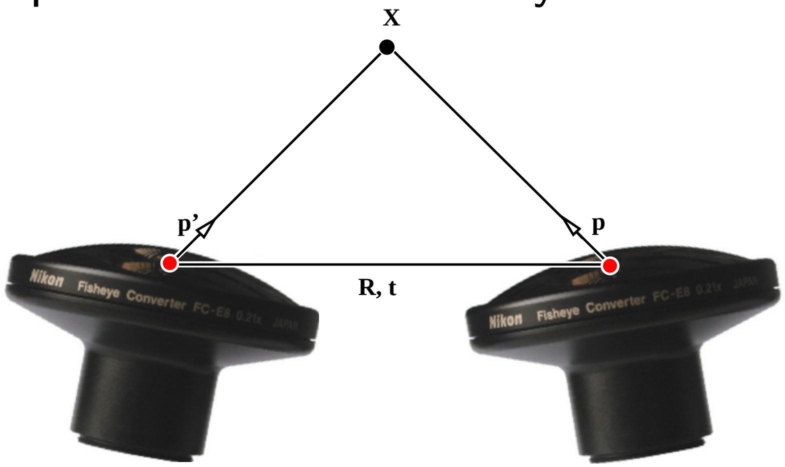

$$\mathbf{p'}^\top \mathtt{F} \mathbf{p} = 0$$

$$(\mathbf{x}' + a\mathbf{s}' + b\mathbf{t}')^\top \mathtt{F} (\mathbf{x} + a\mathbf{s} + b\mathbf{t}) = 0$$

Theory of omnidirectional camera calibration

- Taylor series of g with respect to parameters a, b

$$\mathbf{p} \simeq g(\mathbf{u}) = \begin{pmatrix} \mathbf{u} \\ \frac{r}{\tan \frac{ar}{1+br^2}} \end{pmatrix} \approx \mathbf{x} + a\mathbf{s} + b\mathbf{t}$$

- Epipolar constraint for rays

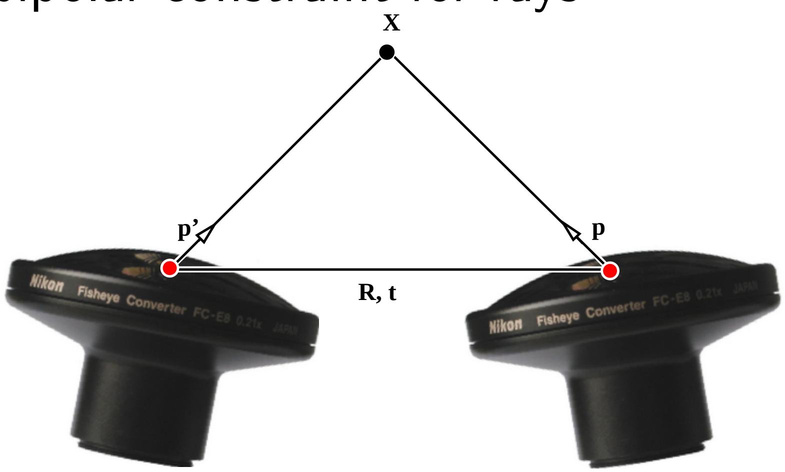

$$\mathbf{p'}^\top \mathtt{F}\mathbf{p} = 0$$

$$(\mathbf{x}' + a\mathbf{s}' + b\mathbf{t}')^\top \mathtt{F}(\mathbf{x} + a\mathbf{s} + b\mathbf{t}) = 0$$

- leads to the Quadratic Eigenvalue Problem (QEP)

$$(\mathtt{D}_1 + a\mathtt{D}_2 + a^2\mathtt{D}_3)\mathbf{h} = 0 \,,$$

where $\mathtt{D_i}$ are known and $\mathbf{h} = [\, f_1 \;\; f_2 \;\; f_3 \;\; f_4 \;\; f_5 \;\; f_6 \;\; f_7 \;\; f_8 \;\; f_9 \;\; bf_3 \;\; bf_6 \;\; bf_7 \;\; bf_8 \;\; bf_9 \;\; b^2f_9 \,]^\top$.

- QEP can be solved by MATLAB using `polyeig`

Results of omnidirectional camera calibration

- the calibrated camera, i.e. the parameters of a nonlinear omnidirectional camera model

$$\theta = \frac{ar}{1+br^2} \quad ,$$

Results of omnidirectional camera calibration

- the calibrated camera, i.e. the parameters of a nonlinear omnidirectional camera model

$$\theta = \frac{ar}{1+br^2},$$

- the essential matrix

$$\mathrm{E} = [\mathbf{t}]_\times \mathrm{R},$$

Results of omnidirectional camera calibration

- the calibrated camera, i.e. the parameters of a nonlinear omnidirectional camera model

$$\theta = \frac{ar}{1+br^2} \; ,$$

- the essential matrix

$$\mathtt{E} = [\mathbf{t}]_\times \mathtt{R} \; ,$$

- correct point correspondences (inliers)

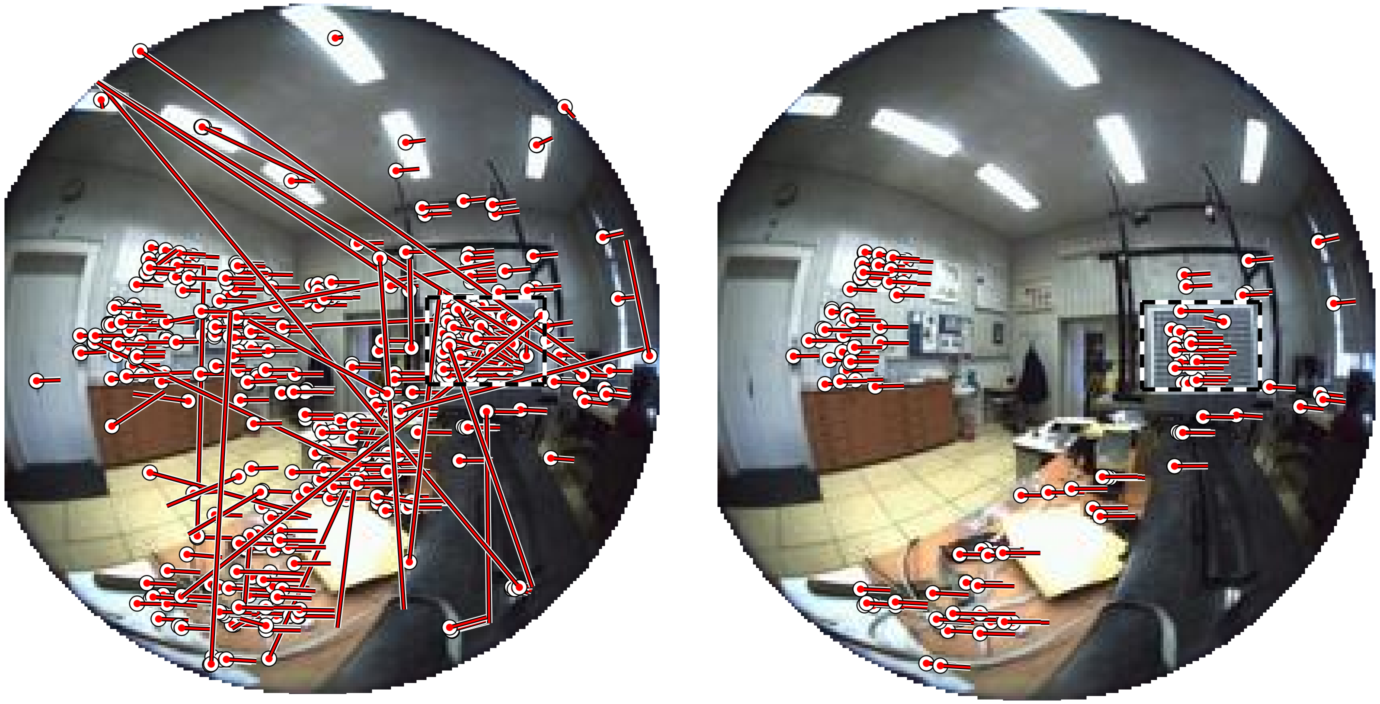

Robust RANSAC-based fitting

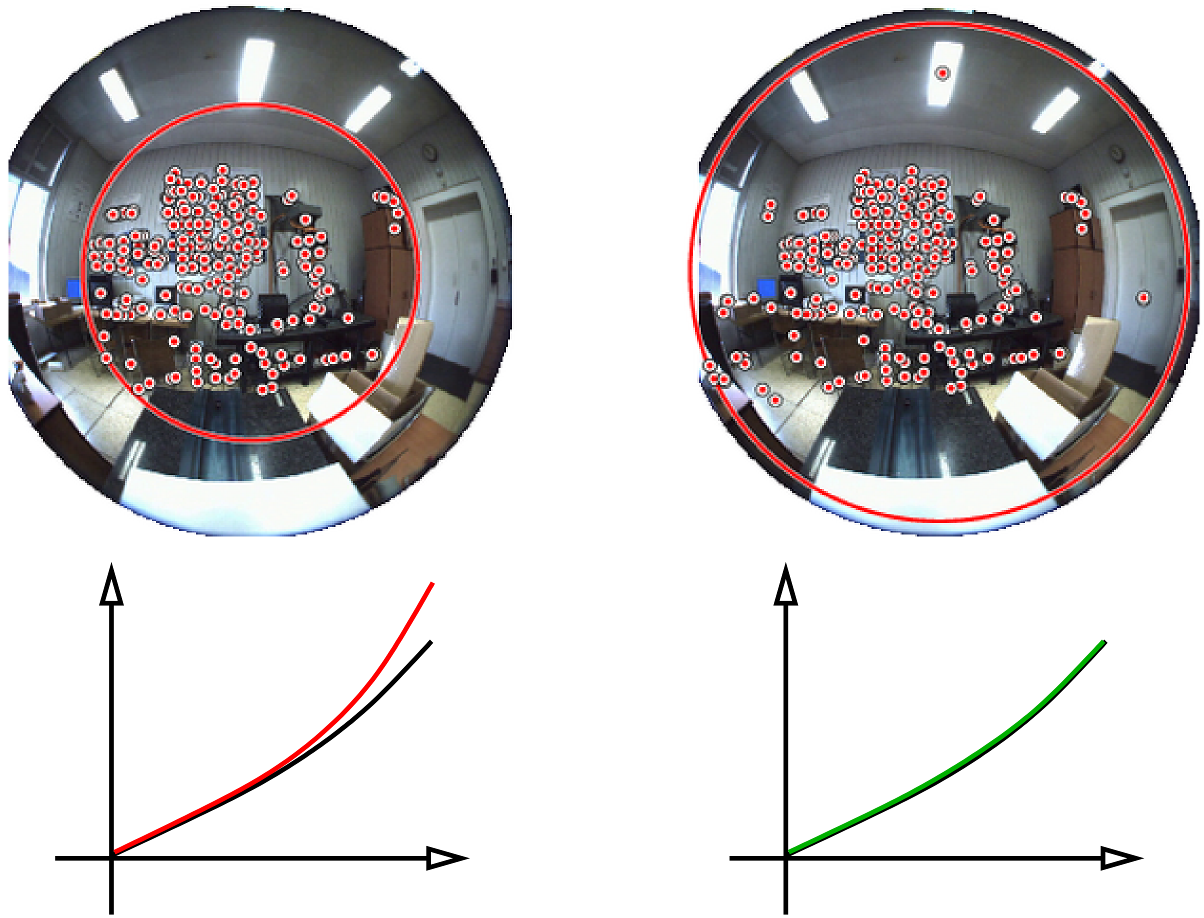

wrong model & EG   correct model & EG

Classical RANSAC:

- RANSAC ends prematurely (even when all correspondences are correct) or
- outliers in the center are selected instead of inliers at the periphery

Robust method based on RANSAC with bucketing

A remedy:

- exclude points near the center from sampling but not from verification
- split the rest of image into three zones with equal areas from which the same number of points are randomly chosen by RANSAC

Robust method based on RANSAC with bucketing

A remedy:

- exclude points near the center from sampling but not from verification
- split the rest of image into three zones with equal areas from which the same number of points are randomly chosen by RANSAC

- The zone sampling can be replaced by more general method based on probability.

Robust method based on RANSAC with bucketing

A remedy:

- exclude points near the center from sampling but not from verification
- split the rest of image into three zones with equal areas from which the same number of points are randomly chosen by RANSAC

- The zone sampling can be replaced by more general method based on probability.
- The zone sampling is straightforward, leads to good results and is sufficient for most of practical situations.

more

Model fitting with tolerance $\Delta\theta$

Why are the points near the center unimportant for the non-linear part of the model?

Model fitting with tolerance $\Delta\theta$

Why are the points near the center unimportant for the non-linear part of the model?

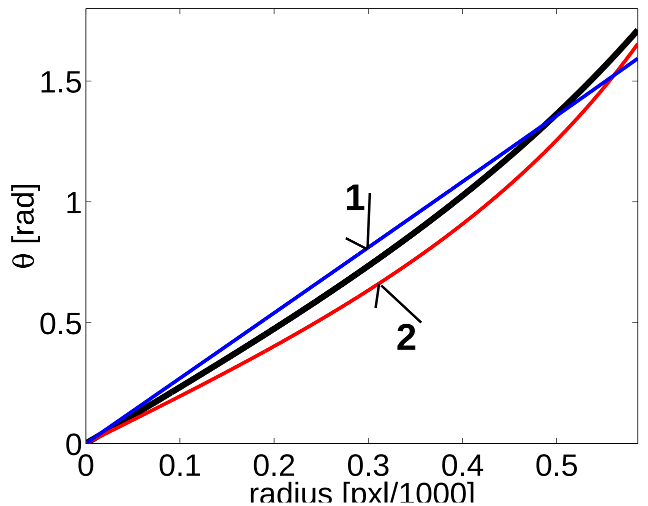

non-linear part of the model

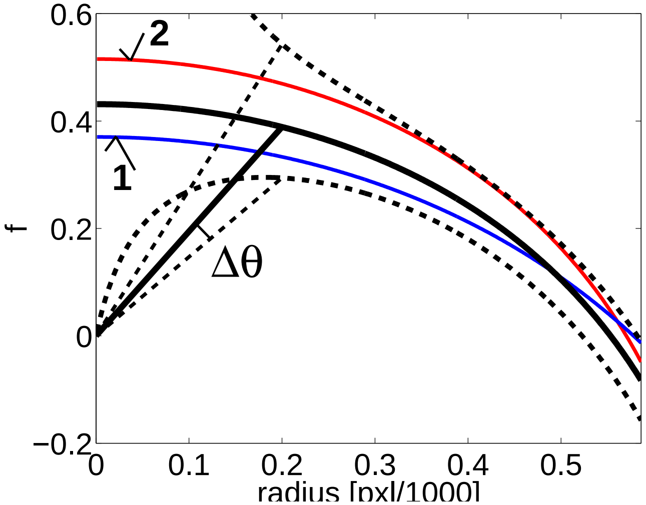

the corresponding f in $\mathbf{p} \simeq (u, v, f)^\top$

- in the center of the image the angular error [Oliensis, PAMI 2002] of a corresponding pair w.r.t. an epipolar plane is insensitive to parameters a,b.

Model fitting with tolerance $\Delta\theta$

Why are the points near the center unimportant for the non-linear part of the model?

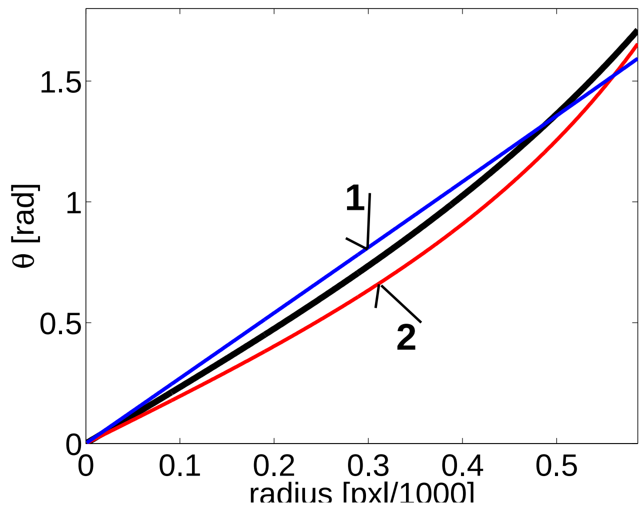

non-linear part of the model

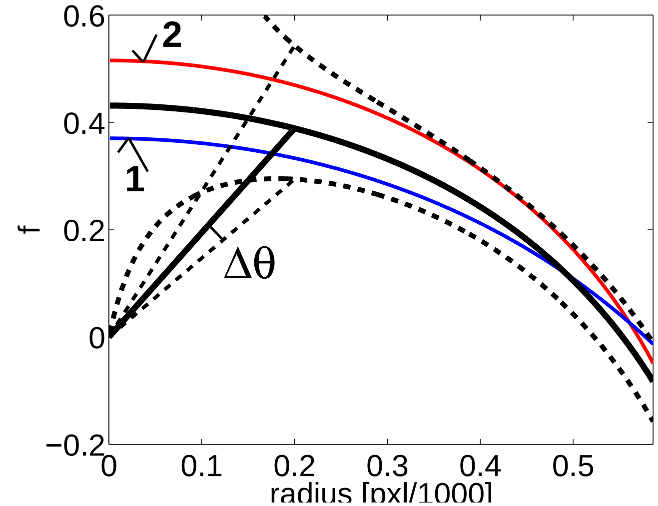

the corresponding f in $\mathbf{p} \simeq (u, v, f)^\top$

- in the center of the image the angular error [Oliensis, PAMI 2002] of a corresponding pair w.r.t. an epipolar plane is insensitive to parameters a,b.
- remark: RANSAC searches for the model & EG which fit the highest number of points within the tolerance $\Delta\theta$

Model fitting with tolerance $\Delta\theta$

Why are the points near the center unimportant for the non-linear part of the model?

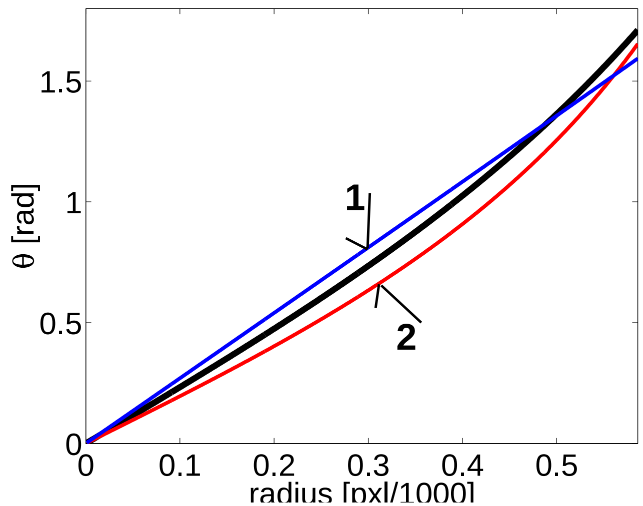

non-linear part of the model

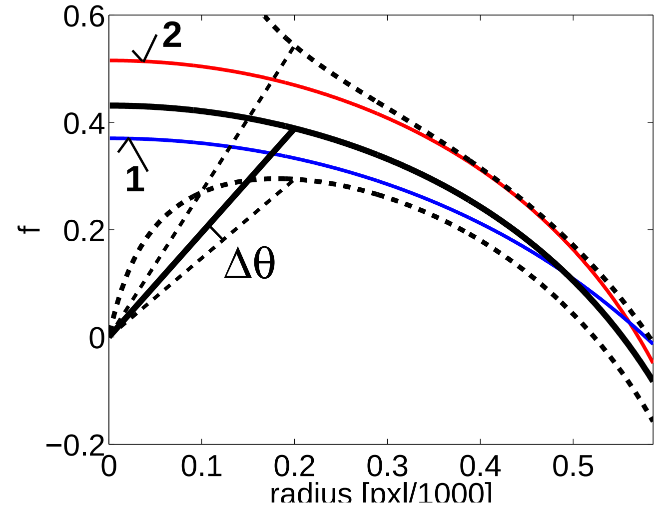

the corresponding f in $\mathbf{p} \simeq (u, v, f)^\top$

- in the center of the image the angular error [Oliensis, PAMI 2002] of a corresponding pair w.r.t. an epipolar plane is insensitive to parameters a,b.
- remark: RANSAC searches for the model & EG which fit the highest number of points within the tolerance $\Delta\theta$
- the most correspondences in the center $\rightarrow$ insensitive to parameters $\rightarrow$ biased estimate

Model fitting with tolerance $\Delta\theta$

Why are the points near the center unimportant for the non-linear part of the model?

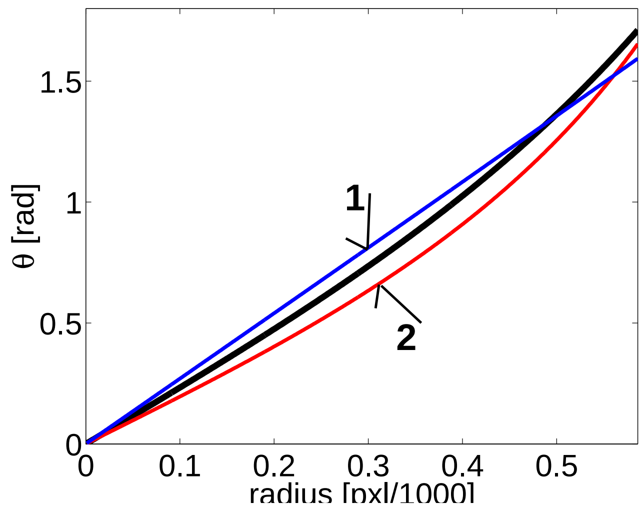

non-linear part of the model

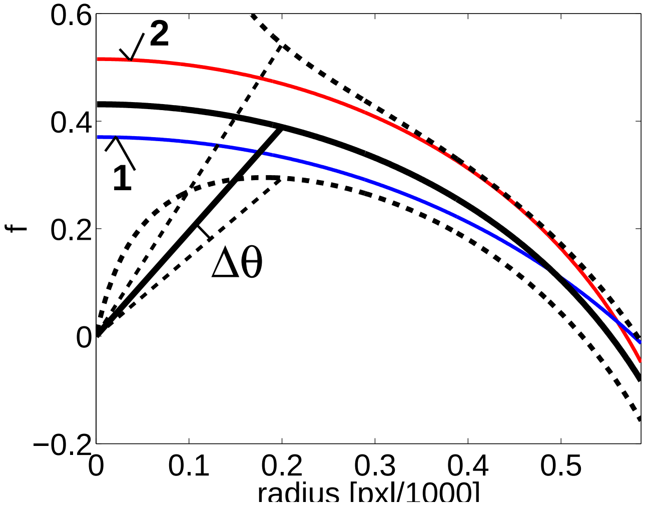

the corresponding f in $\mathbf{p} \simeq (u, v, f)^\top$

- in the center of the image the angular error [Oliensis, PAMI 2002] of a corresponding pair w.r.t. an epipolar plane is insensitive to parameters a,b.
- remark: RANSAC searches for the model & EG which fit the highest number of points within the tolerance $\Delta\theta$
- the most correspondences in the center $\rightarrow$ insensitive to parameters $\rightarrow$ biased estimate
- Remedied by sampling with bucketing

more

APPLICATIONS

Image projection into a sphere

- Calibration available

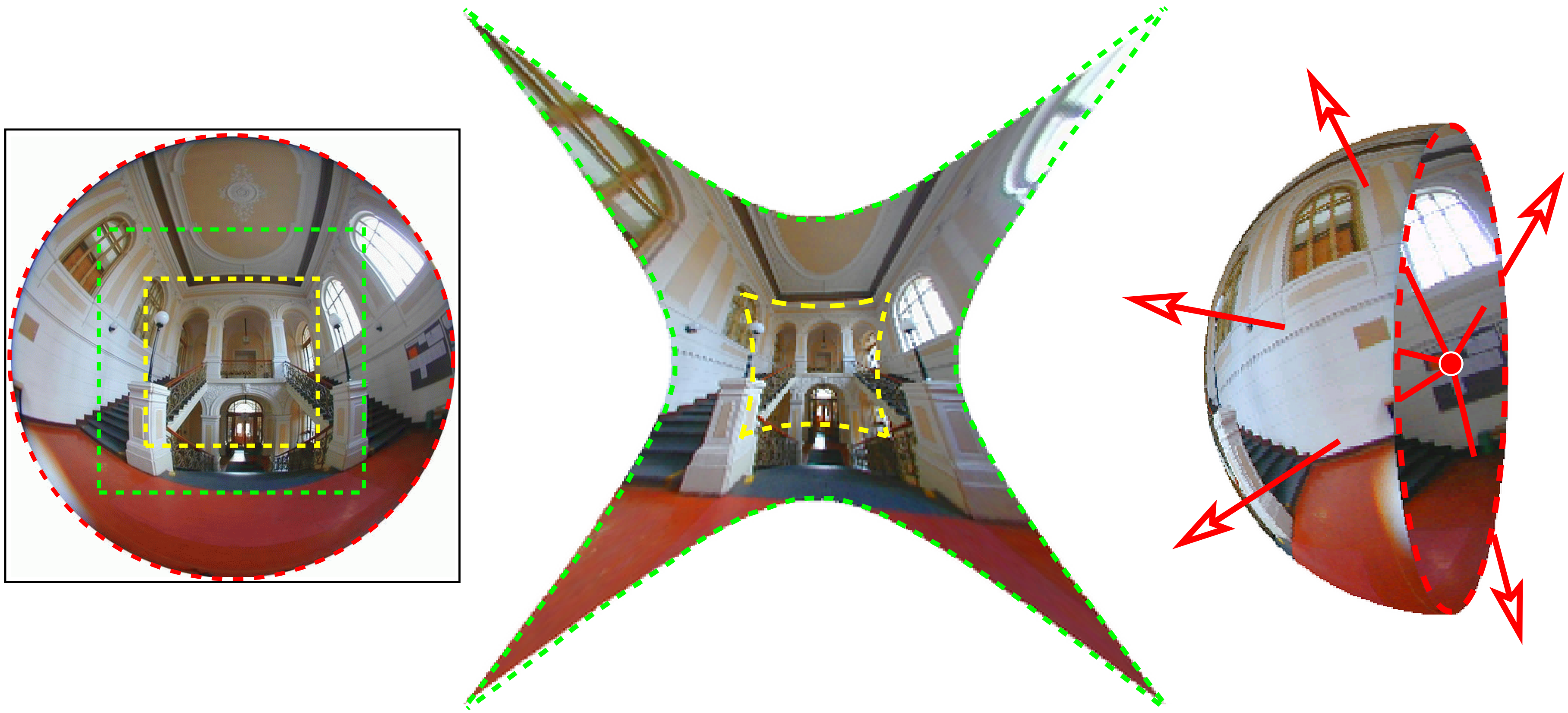

- a perspective image can be generated only for a limited (e.g. $< 160^\circ$) field of view
- the whole image can be represented on a sphere

Trajectory estimation

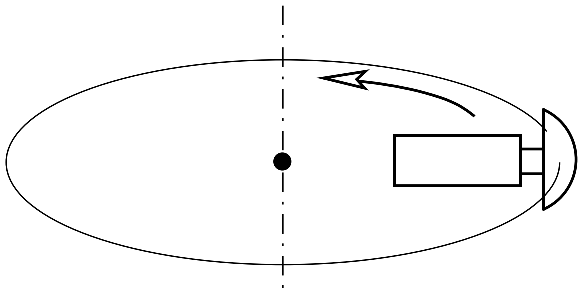

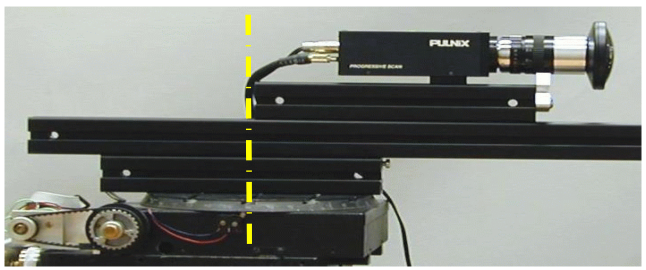

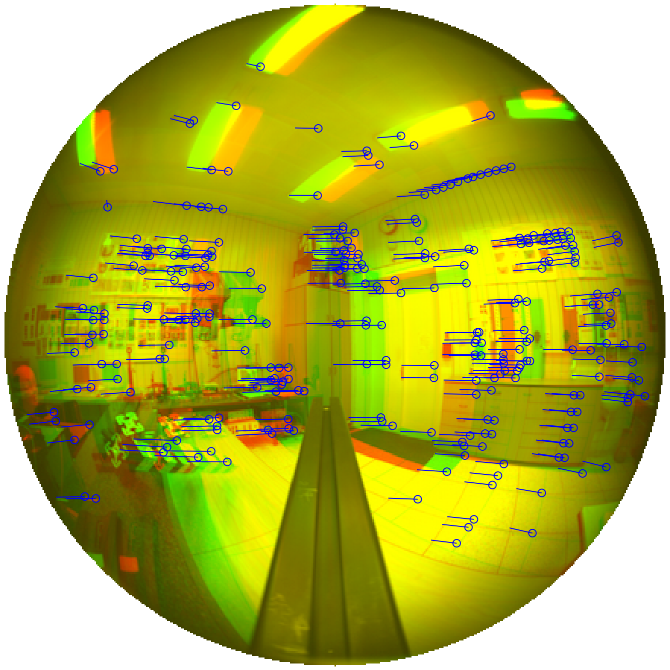

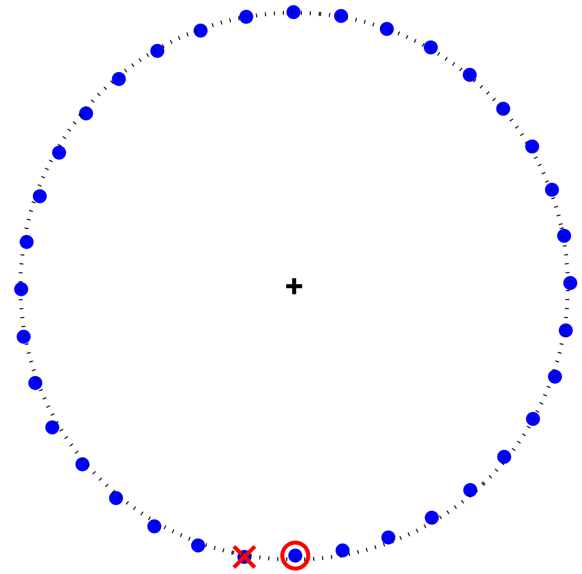

- Nikon FC–E8 lens mounted on a digital camera with resolution 1017$\times$1008 pxls was rotated along a circle, correspondences obtained by *boujou*, 2d3 Ltd.
- relative camera rotations and directions of translations are computed from essential matrices

Trajectory estimation

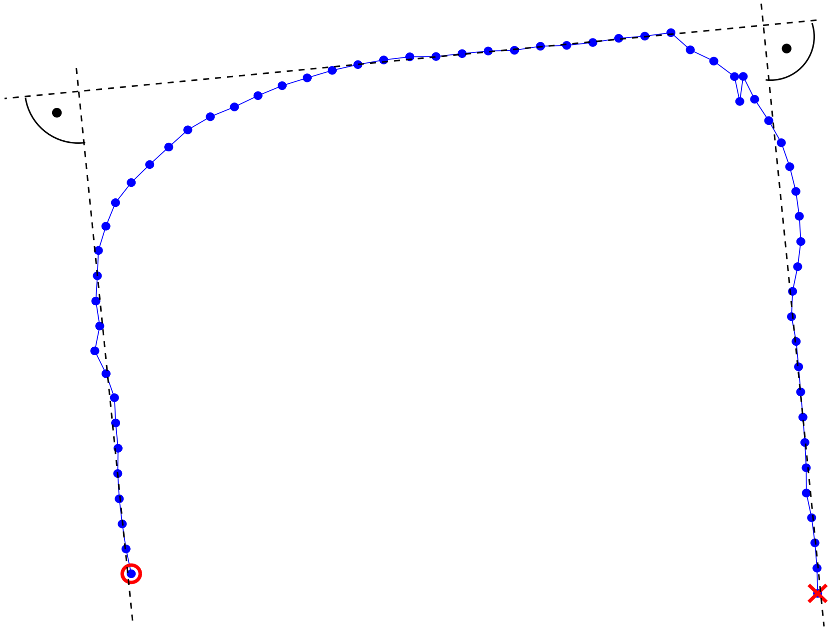

- general motion experiment
- the estimated trajectory with starting and ending directions that are mutually parallel

more

3D Metric reconstruction

(In collaboration with Daniel Martinec, CMP Prague)

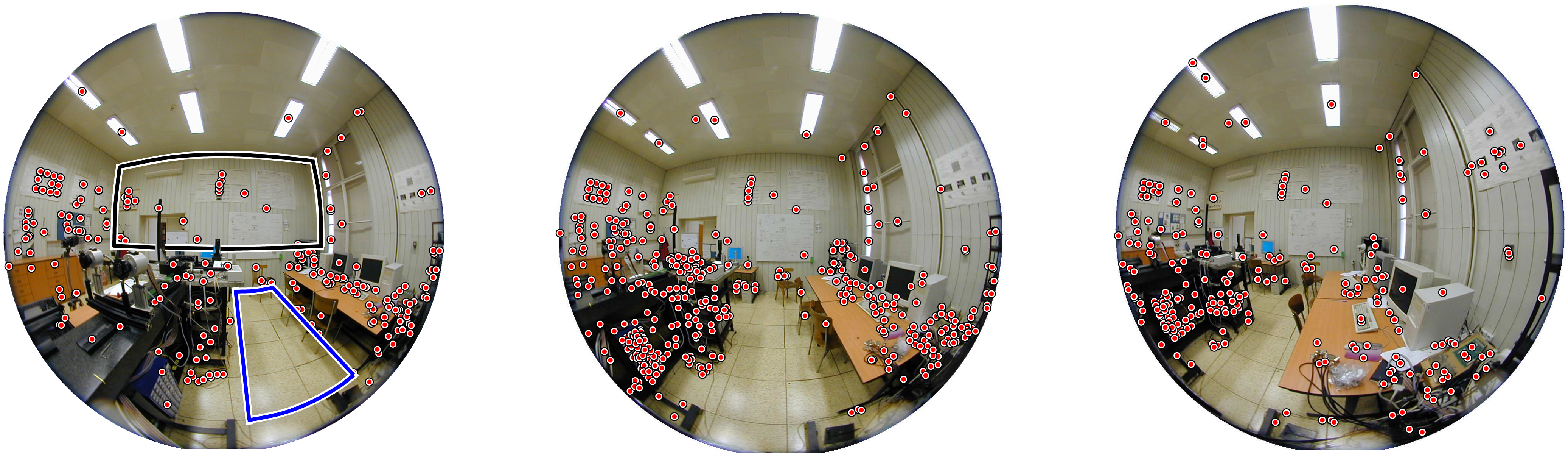

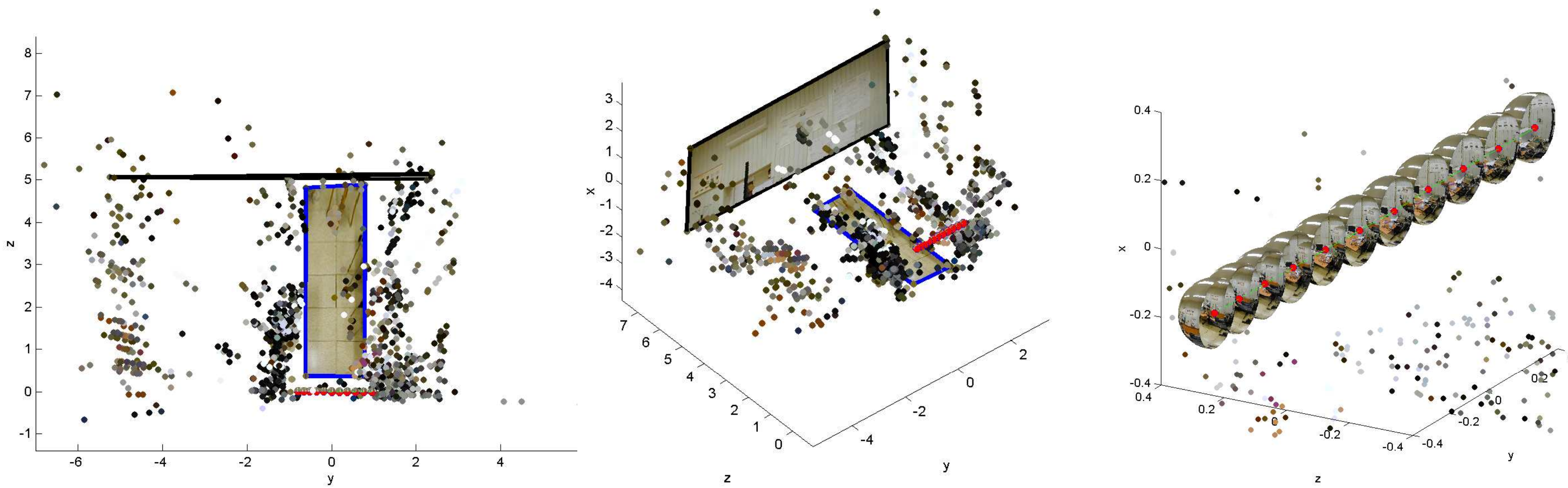

Conclusion

Main contribution:

- Epipolar geometry estimation and
- omnidirectional camera calibration
- by RANSAC with bucketing
- for very wide-angle ($> 180°$) of view
- from point correspondences.

Conclusion

Main contribution:

- Epipolar geometry estimation and
- omnidirectional camera calibration
- by RANSAC with bucketing
- for very wide-angle ($> 180°$) of view
- from point correspondences.

Remarks:

- It is the number of parameters, rather than the actual form of the non-linear function, what allows to formulate the calibration process as QEP
- Experiments show that
  - more complete 3D reconstruction from fewer omnidirectional images
  - large field of view $\rightarrow$ very stable results even without bundle adjustment
  - suitable model + linearization + QEP $\rightarrow$ solves large class of lenses and mirrors

m p

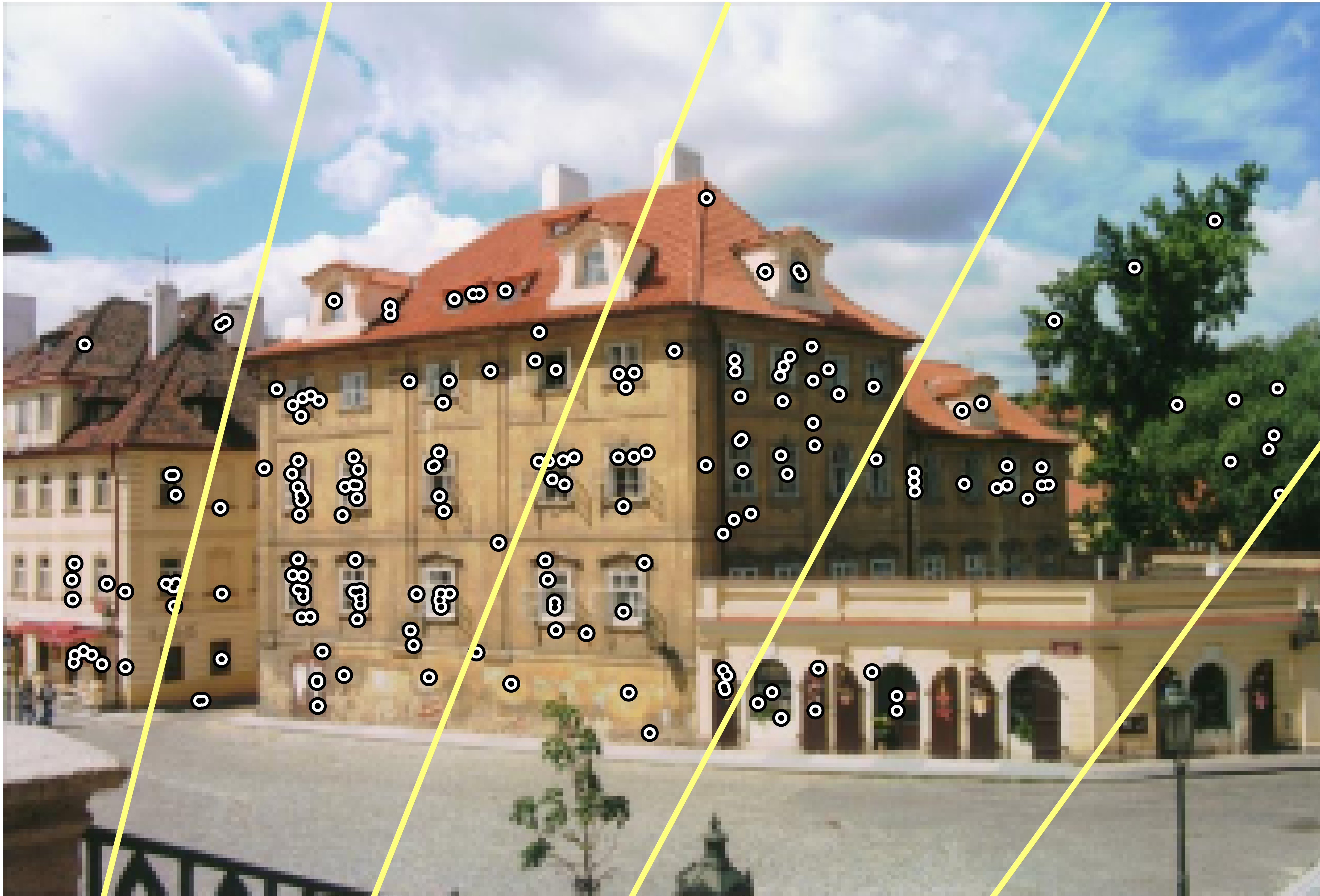

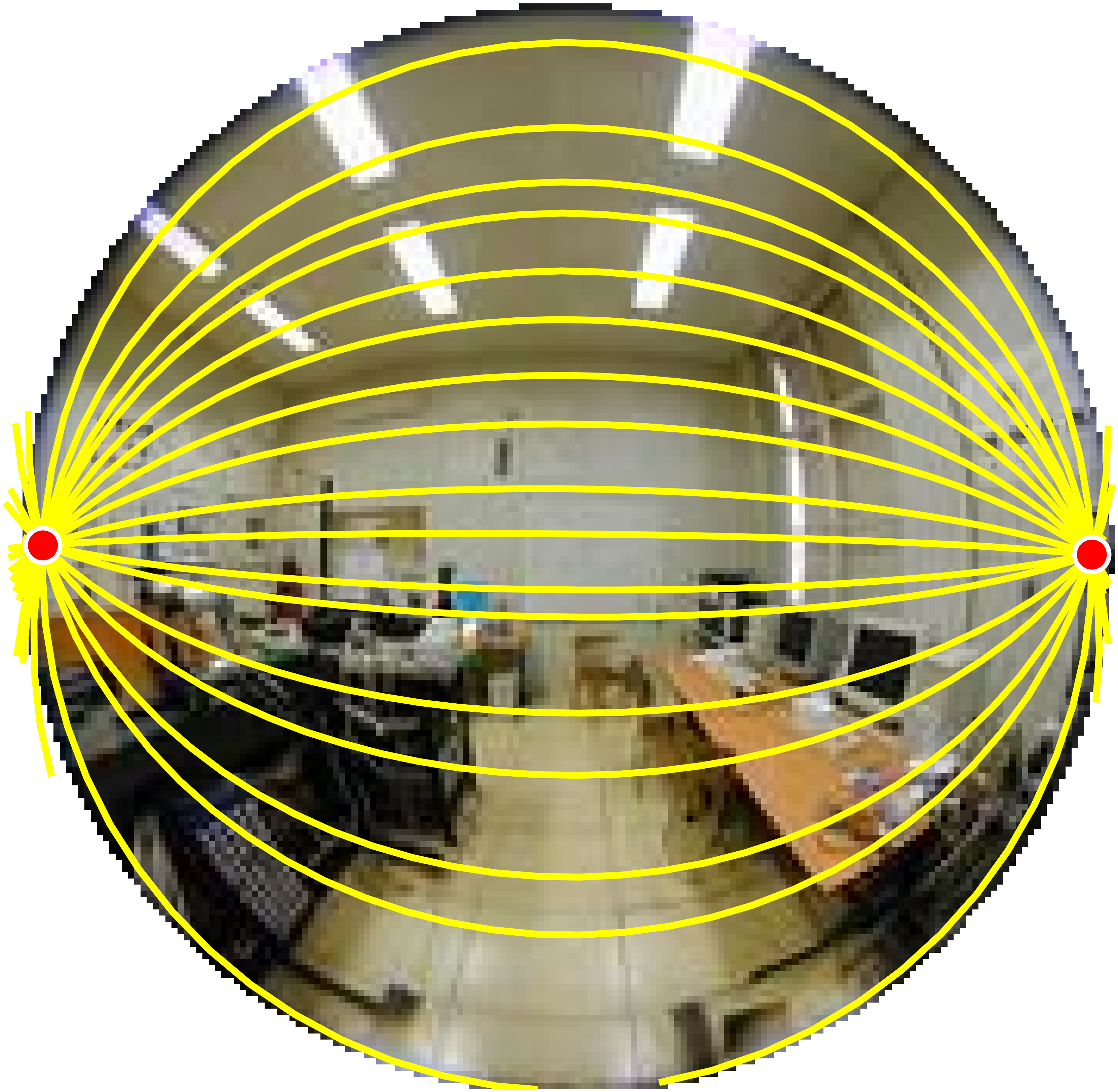

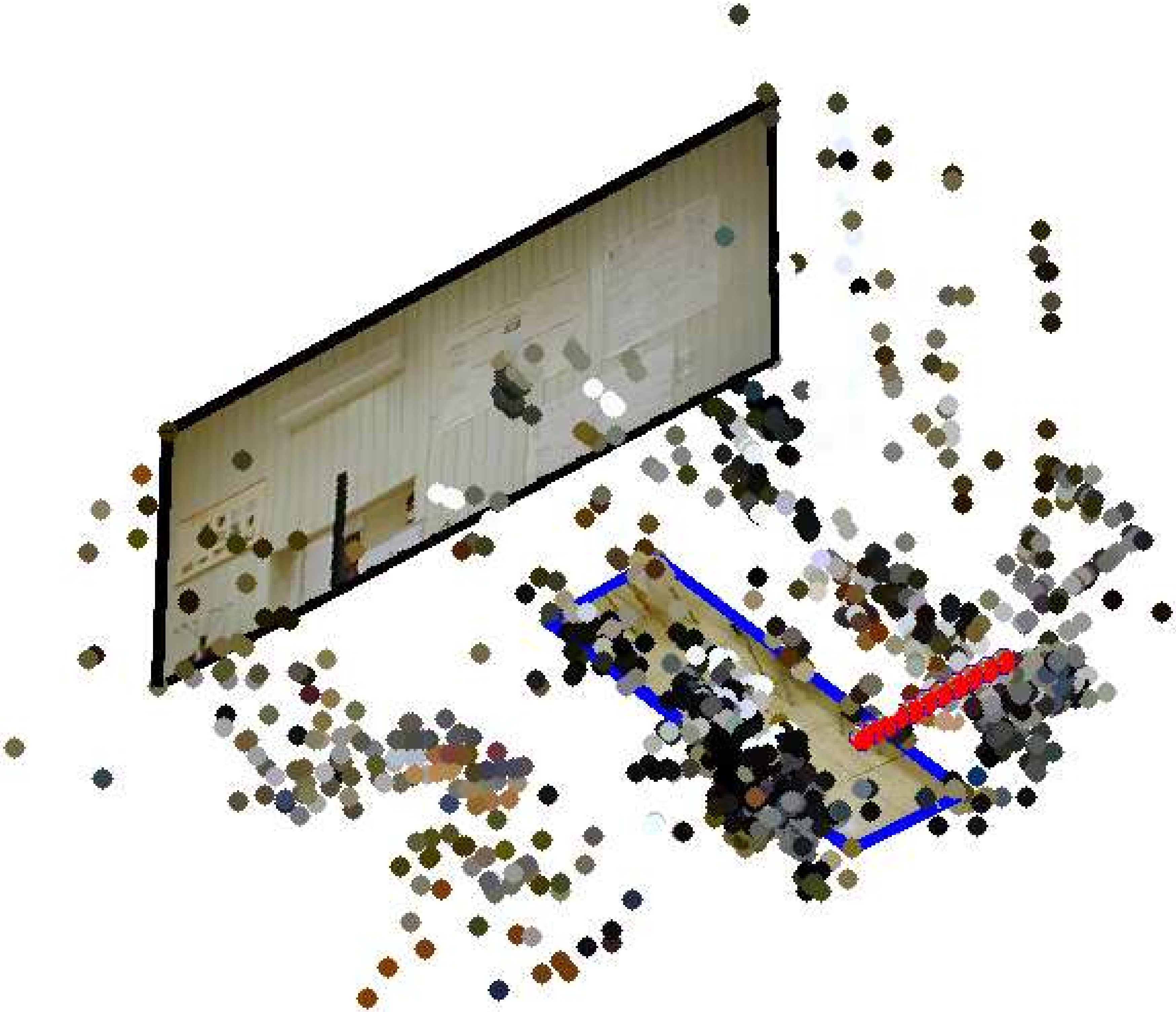


OMNIVIEWS

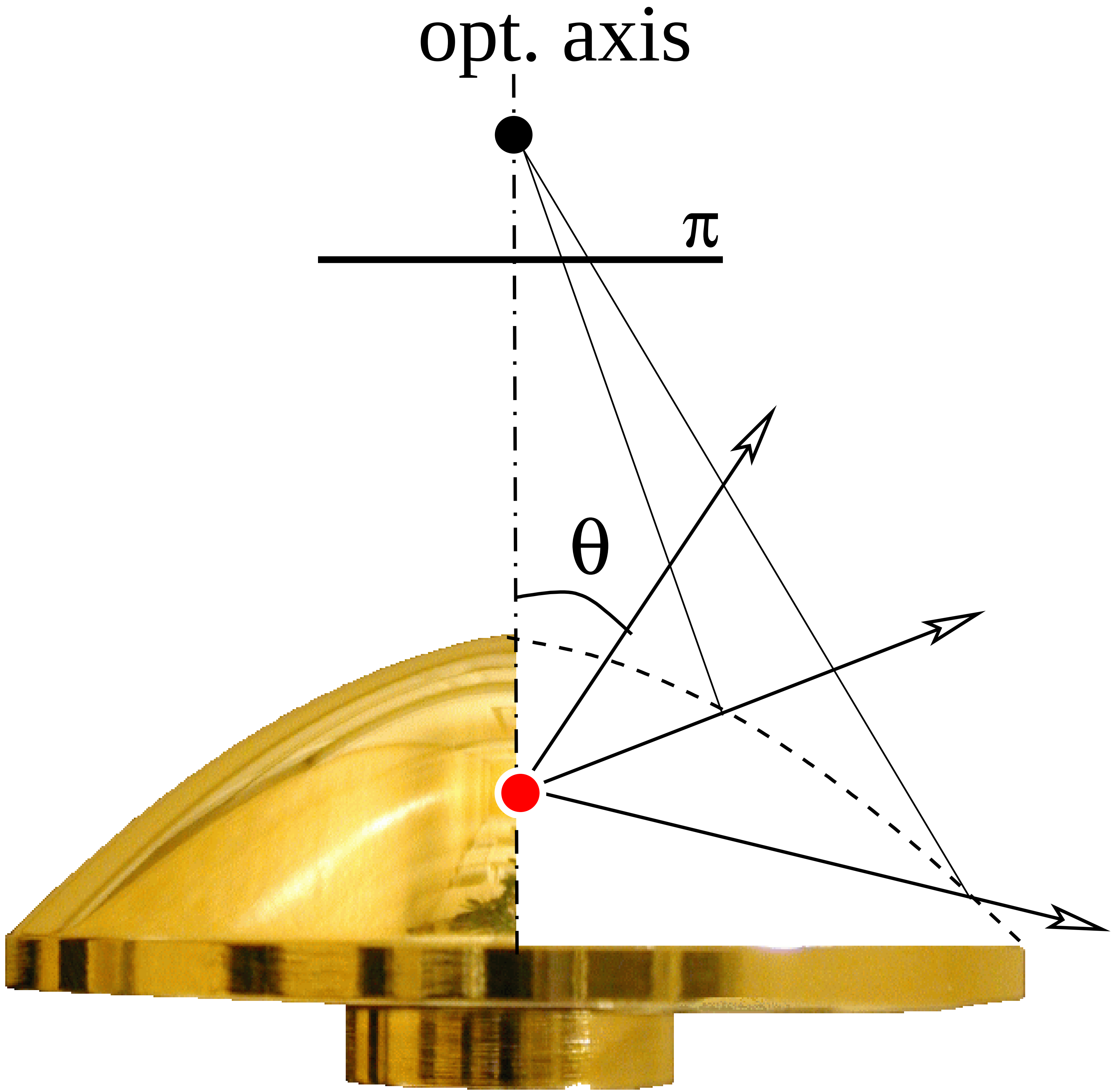

opt. axis
π
θ


Nikon

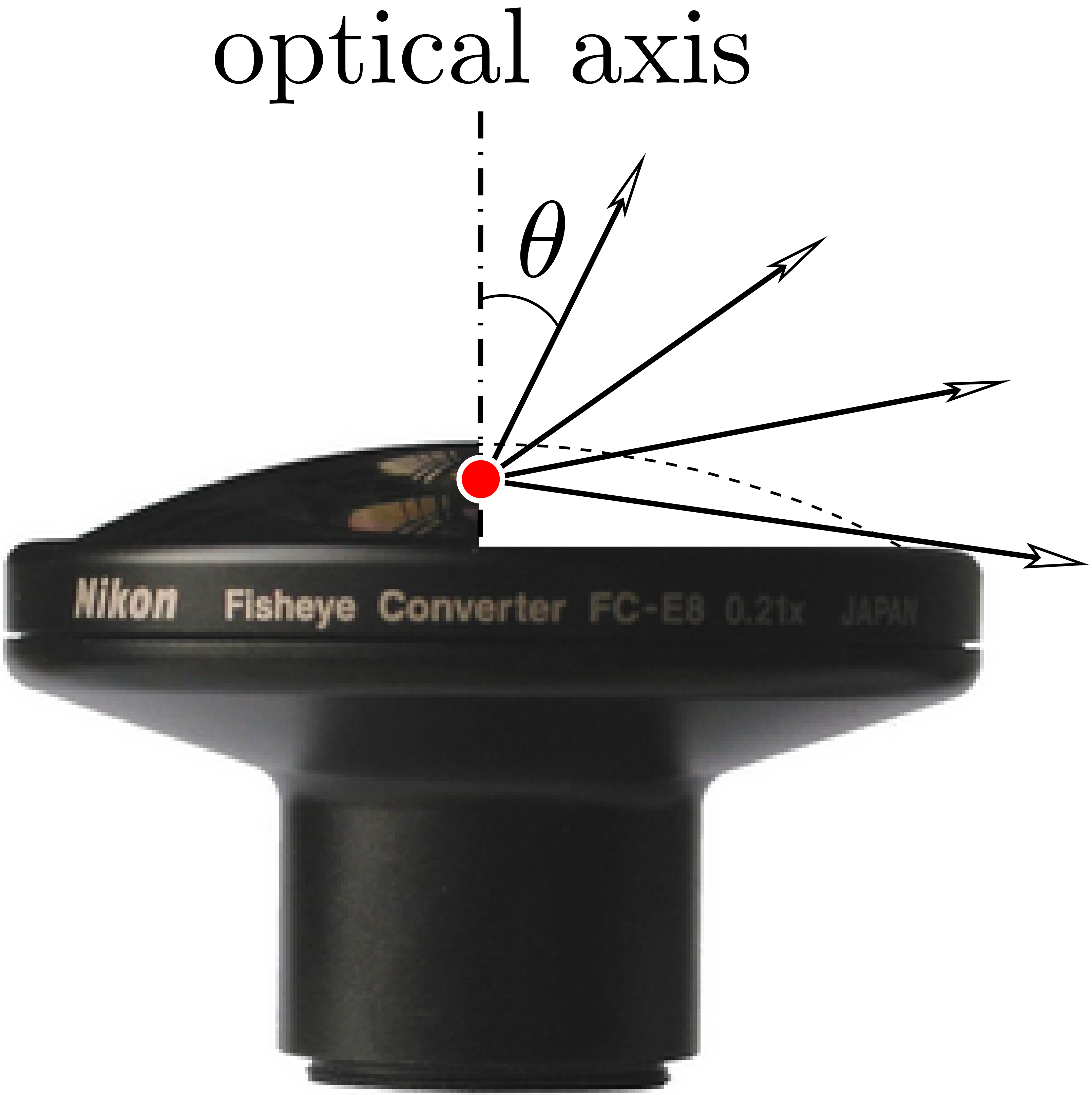
optical axis
θ
Nikon Fisheye Converter FC-E8 0.21x JAPAN

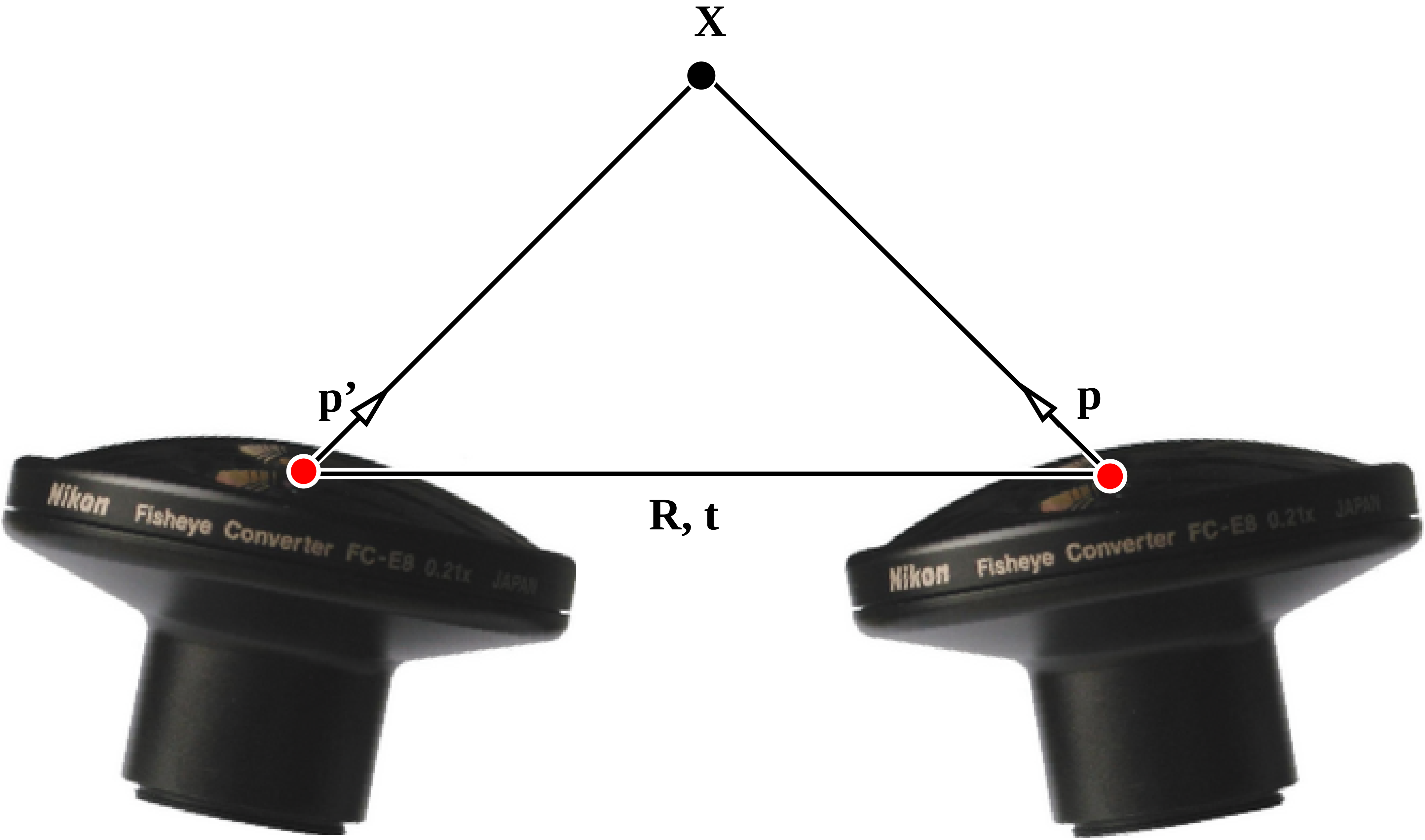

X
p’
p
R, t
Nikon Fisheye Converter FC-E8 0.21x JAPAN
Nikon Fisheye Converter FC-E8 0.21x JAPAN

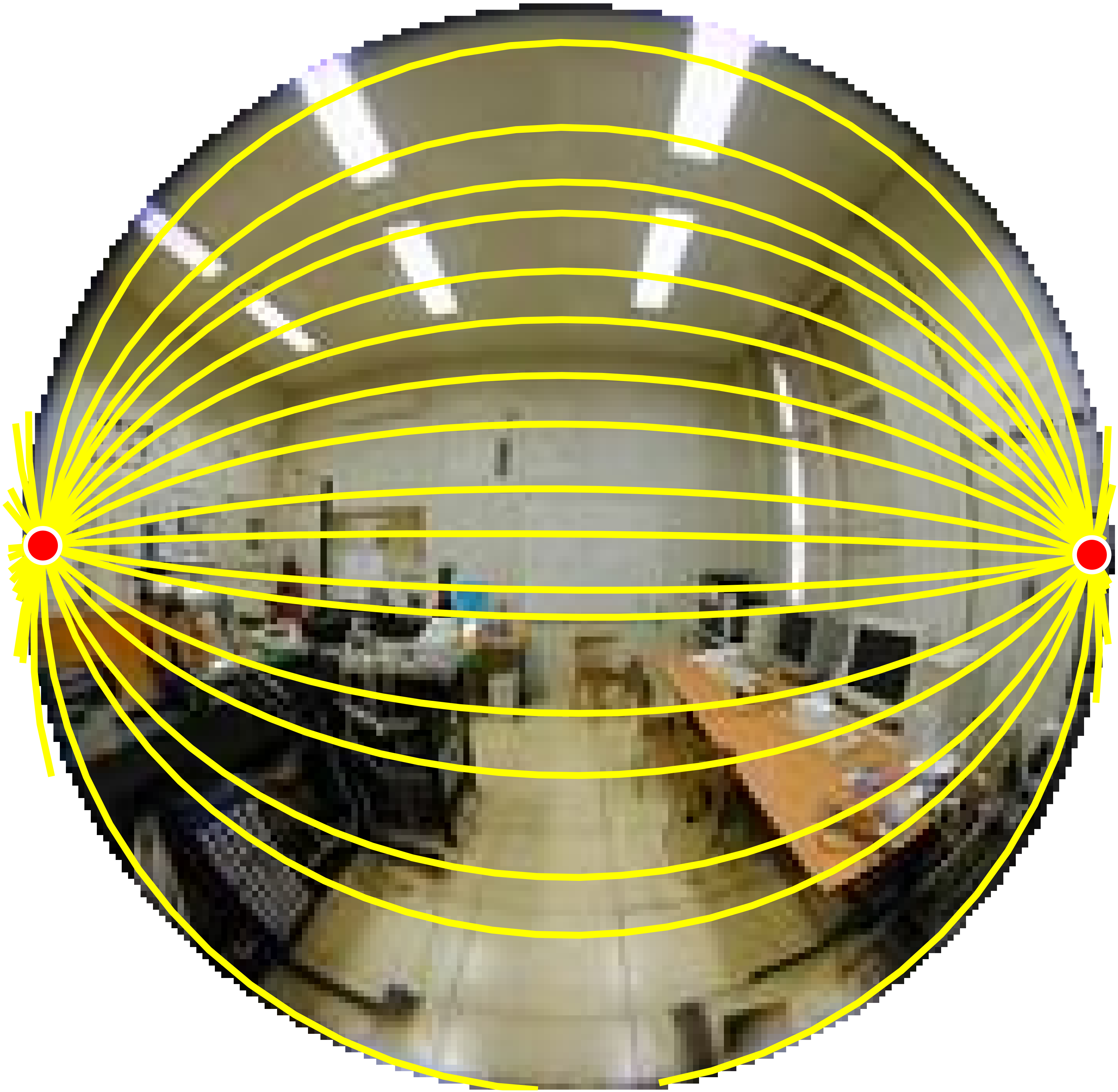


PULNiX
PROGRESSIVE SCAN


u

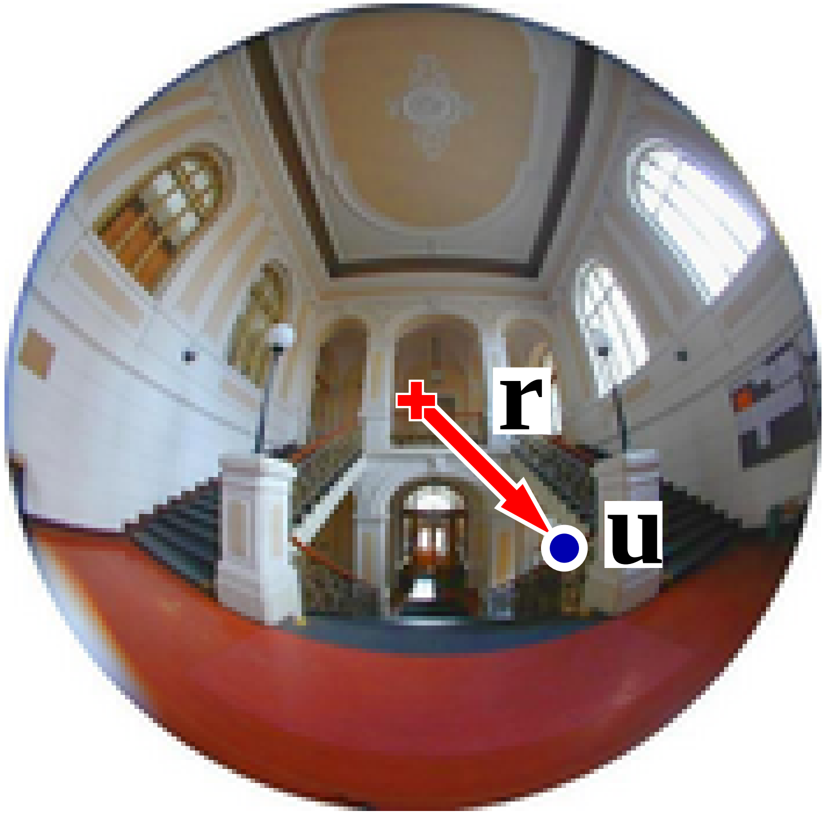
r
u


p
θ
r
u


p
θ
r
u

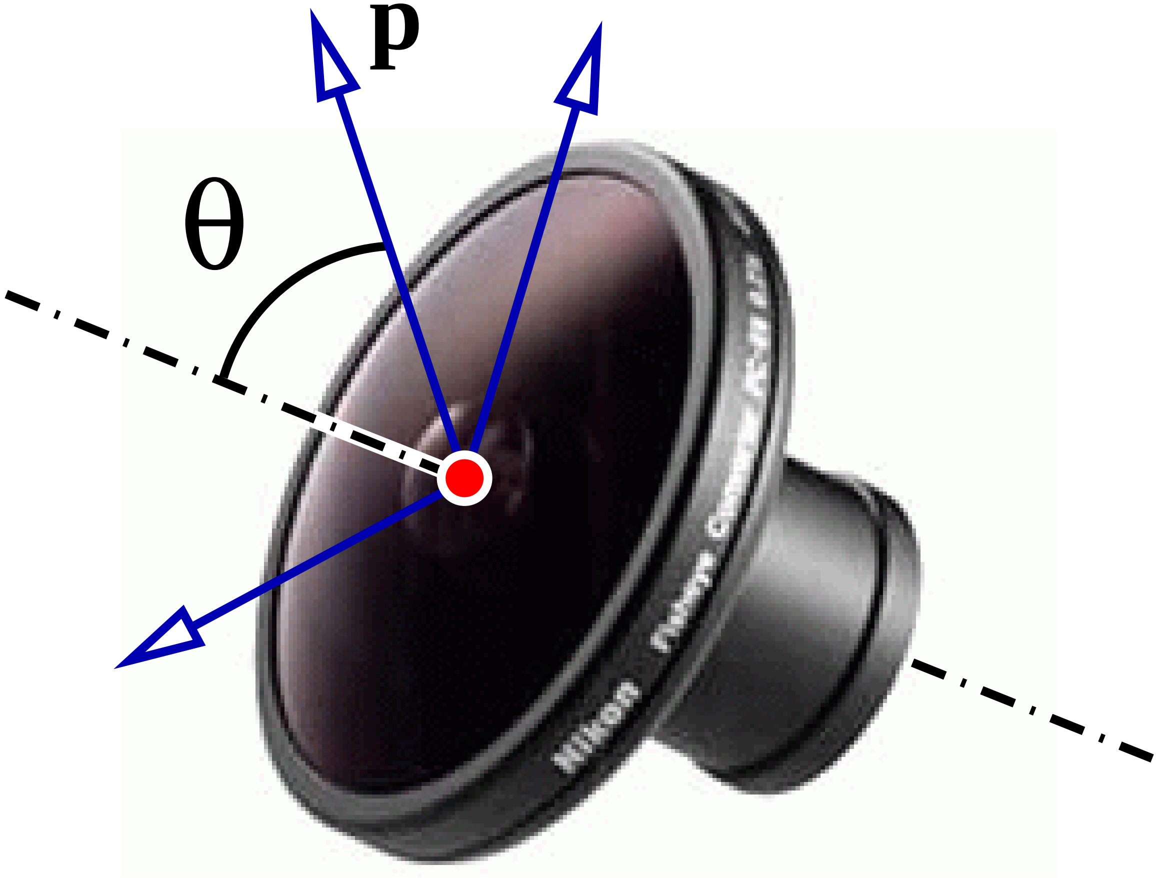
p
θ

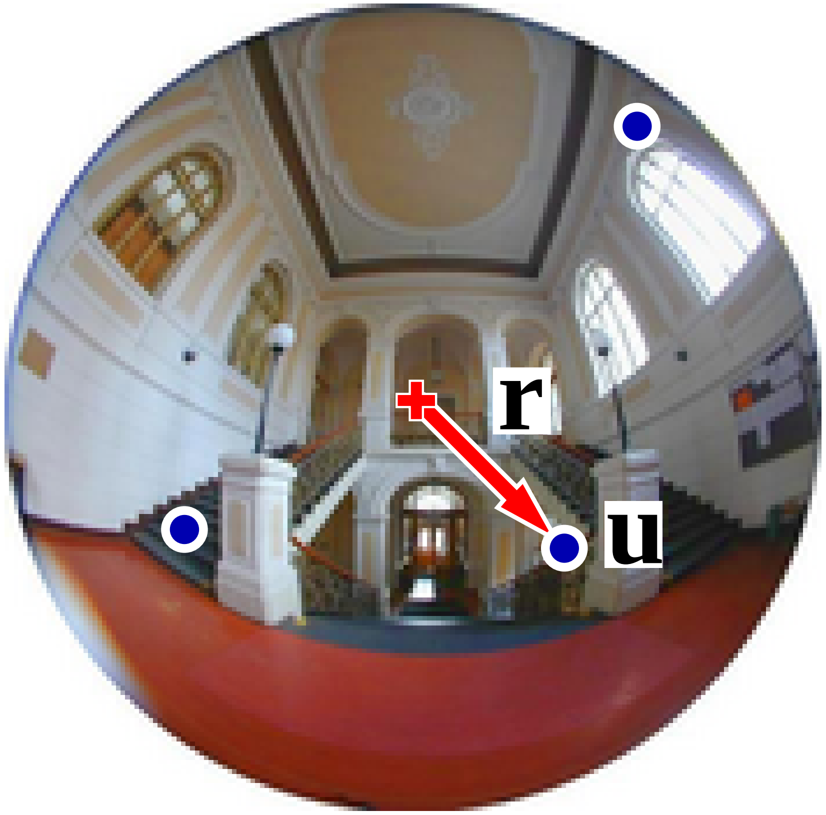
r
u


u


r
u


p
θ
r
u


p
θ
r
u

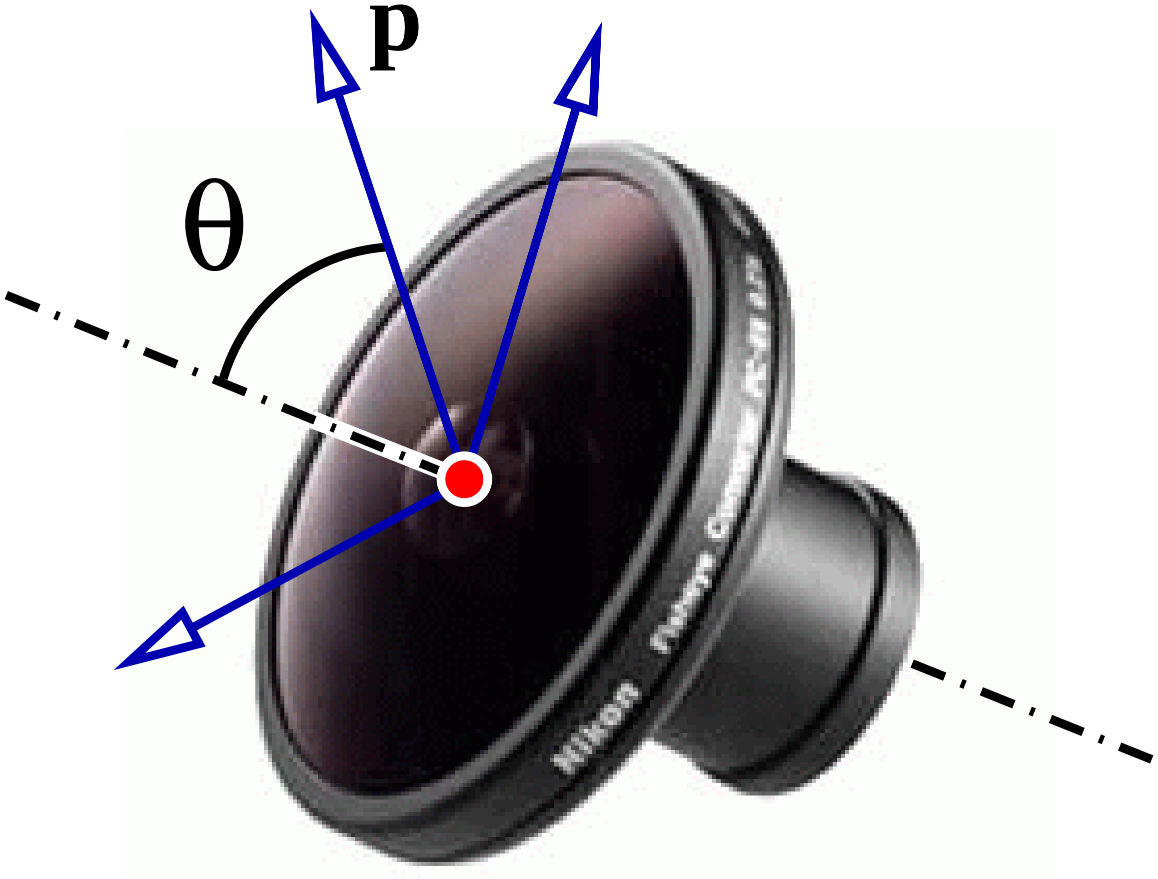
p
θ

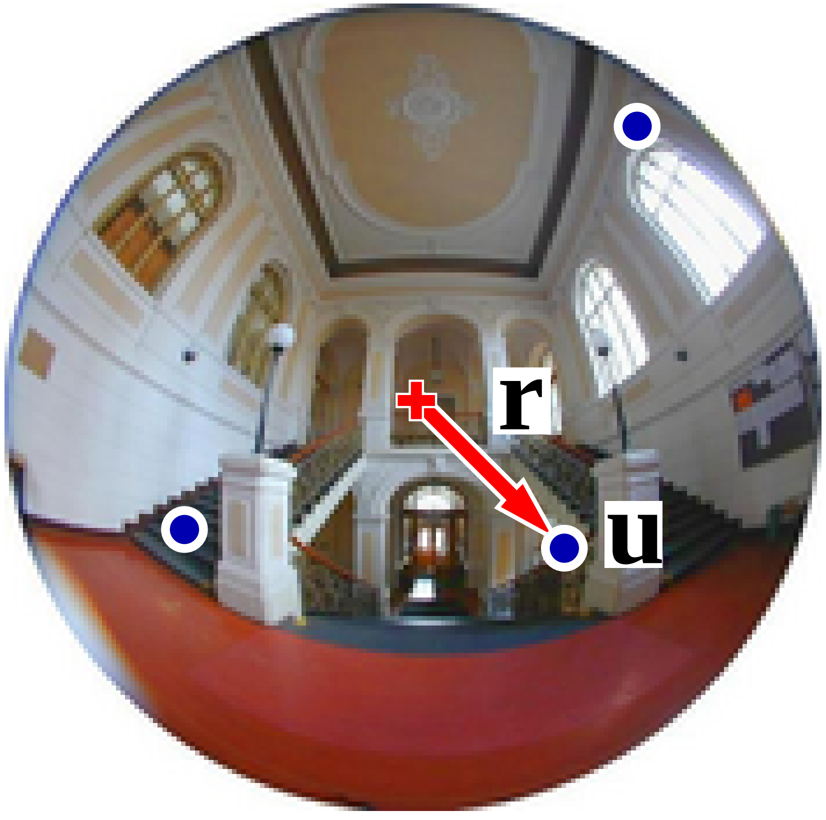
r
u

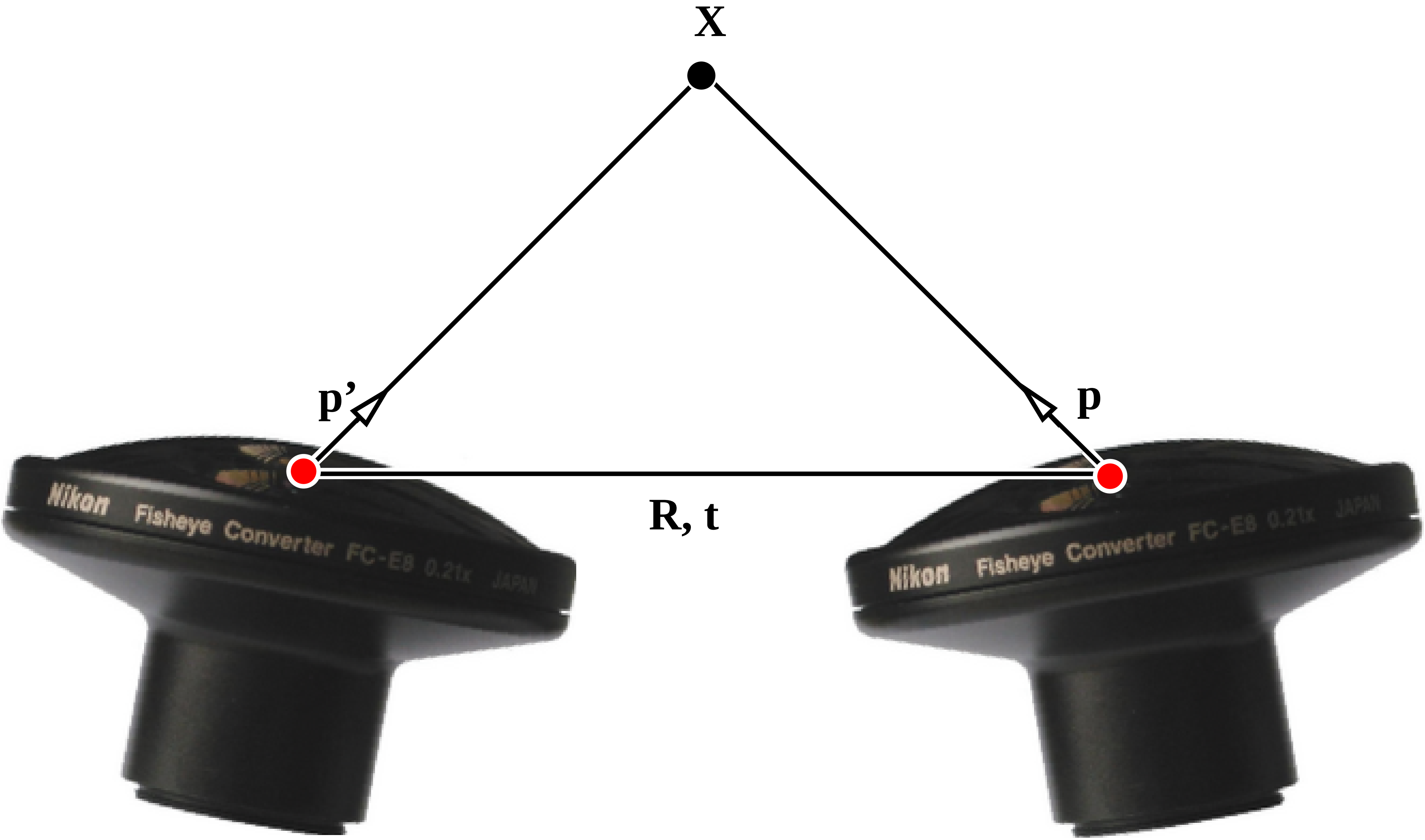
X
p'
p
R, t
Nikon Fisheye Converter FC-E8 0.21x JAPAN
Nikon Fisheye Converter FC-E8 0.21x JAPAN

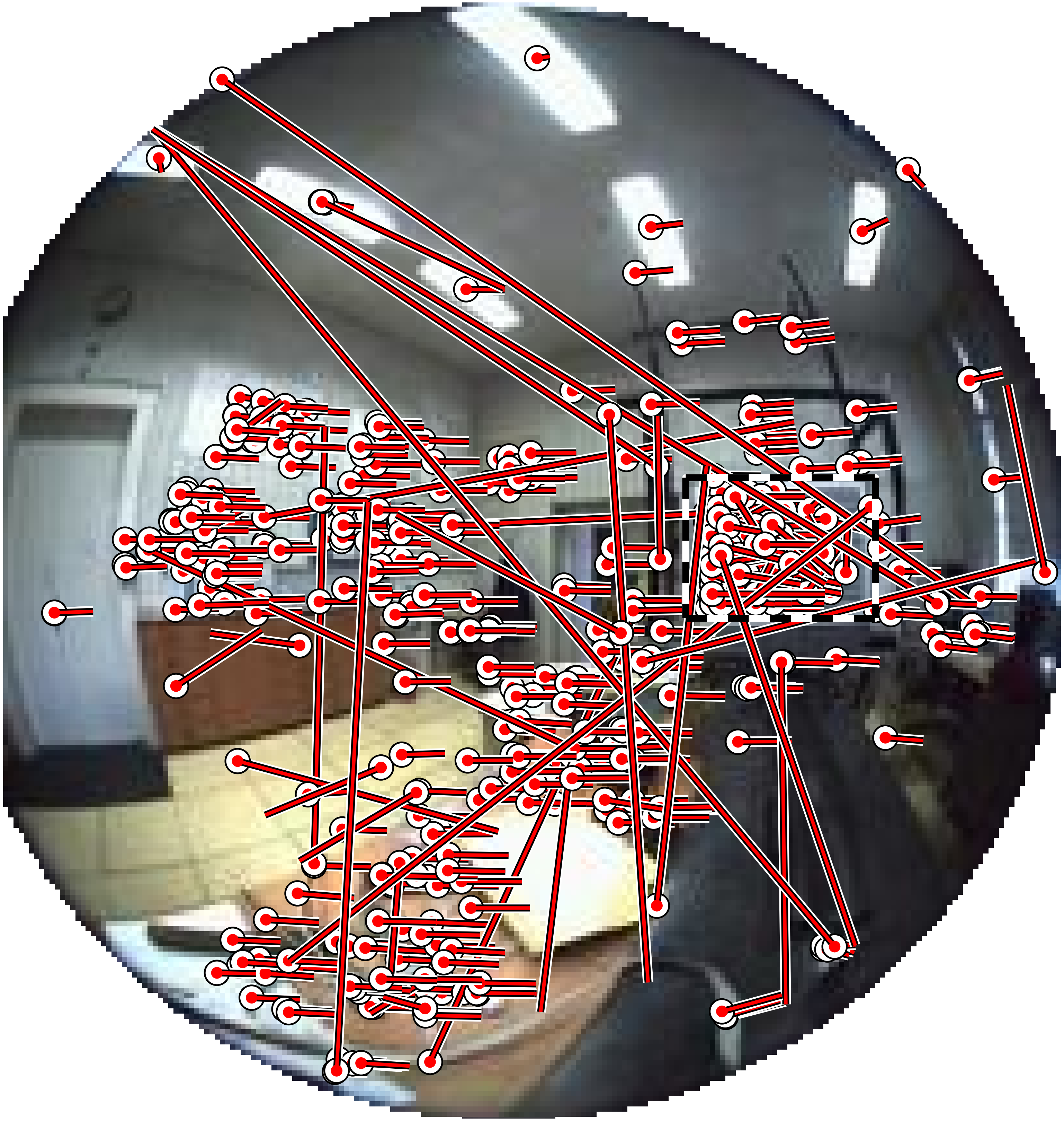

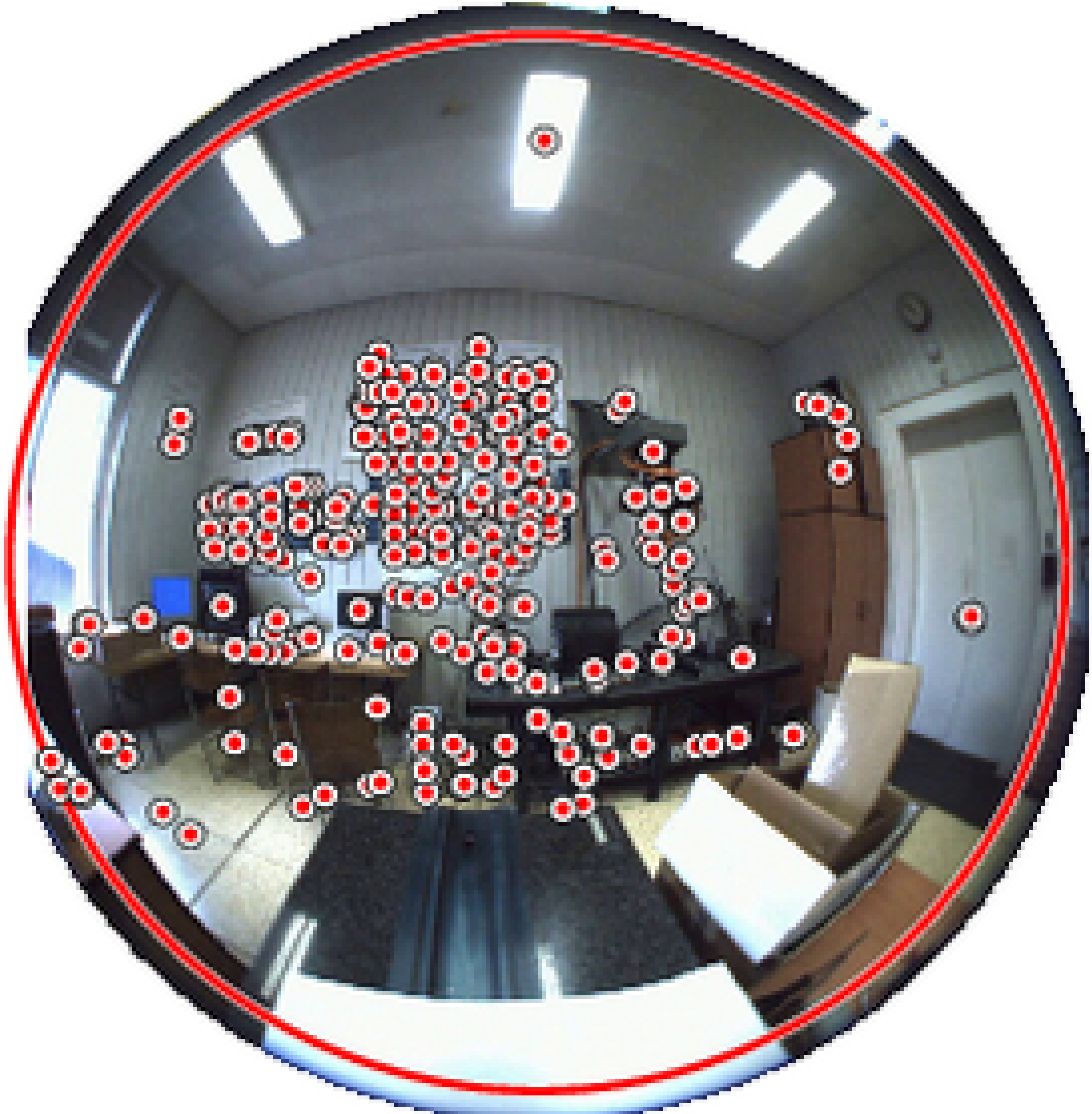

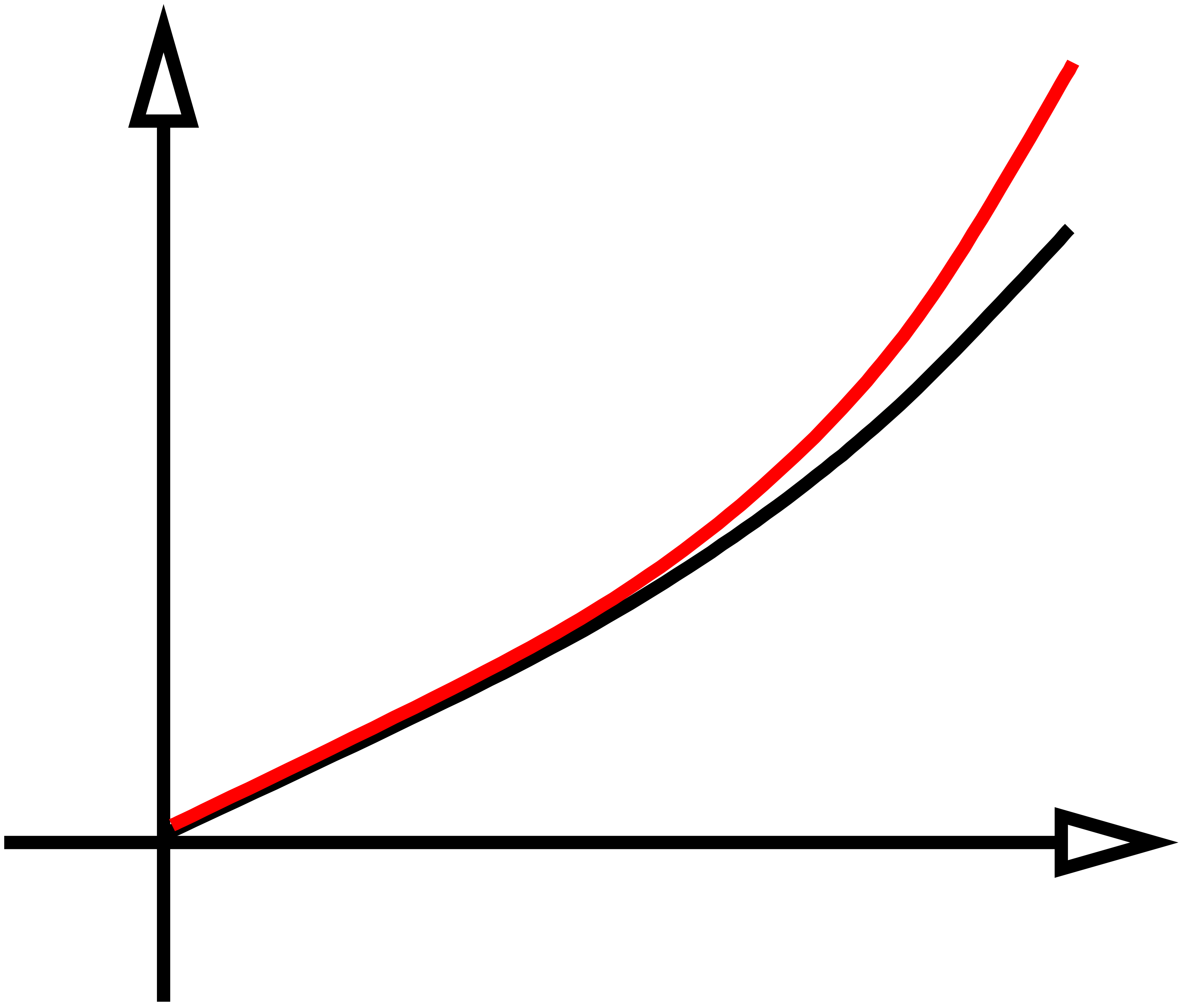

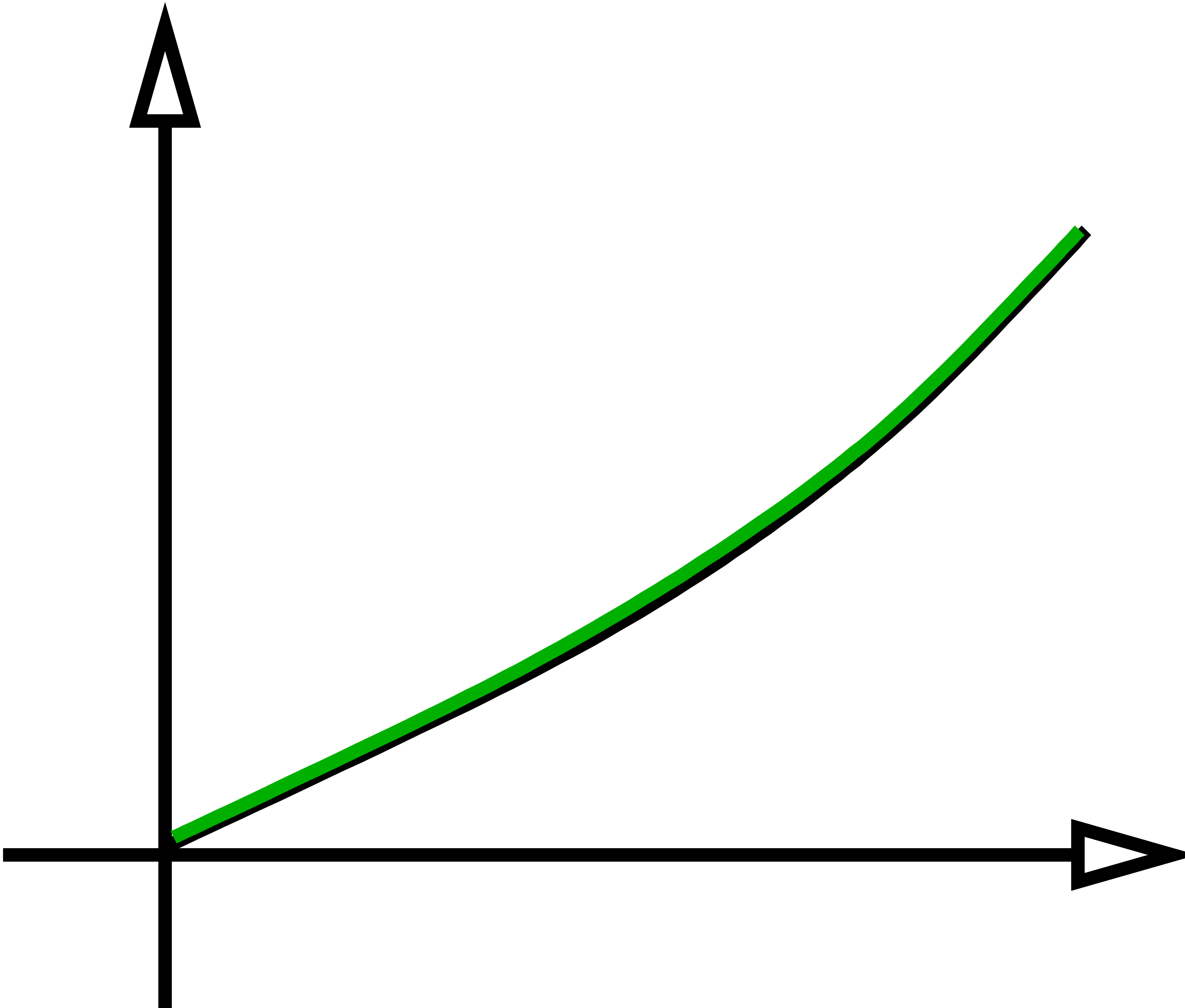

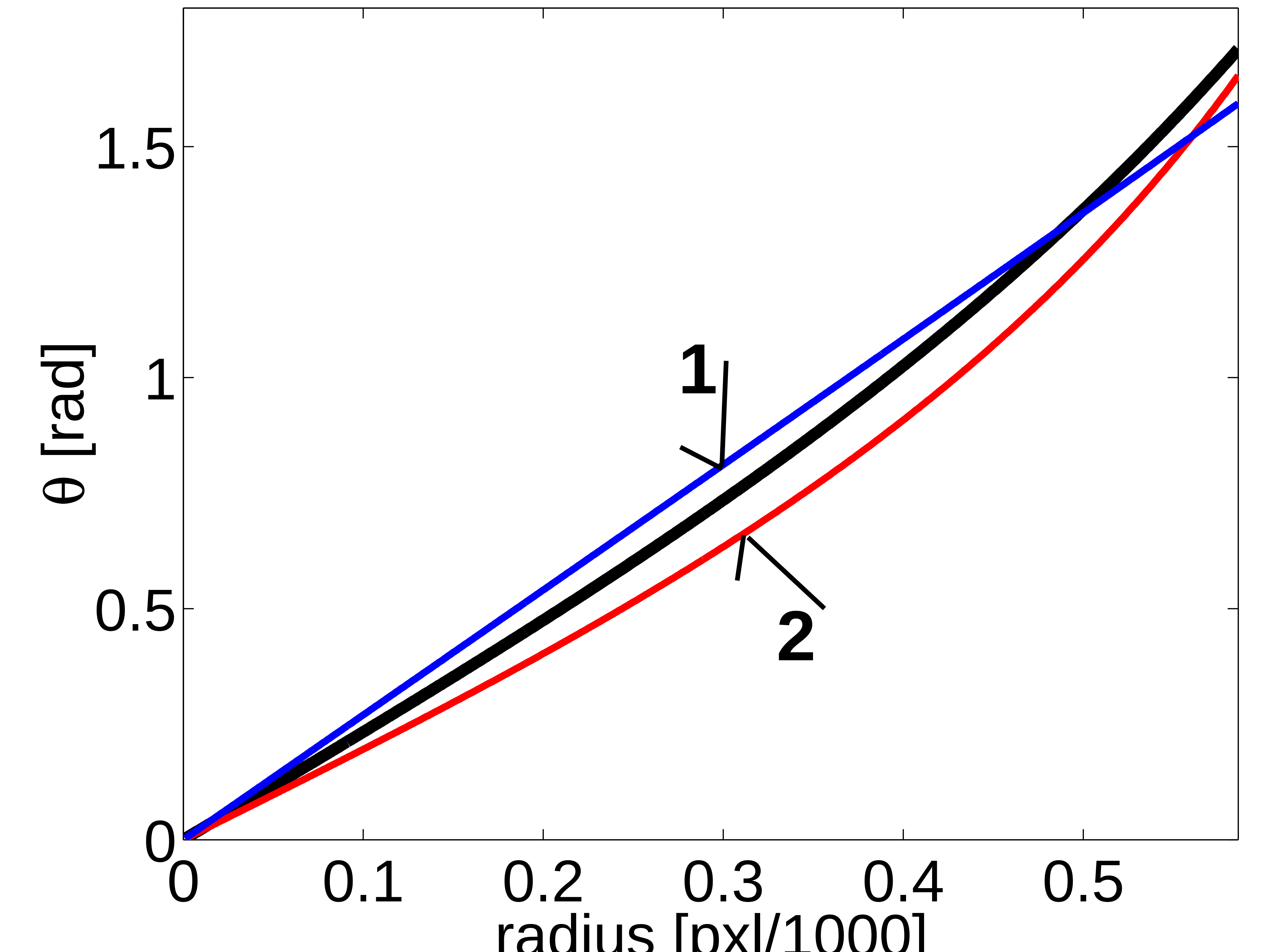

1.5
1
0.5
0
θ [rad]
0
0.1
0.2
0.3
0.4
0.5
radius [px]/1000]
1
2

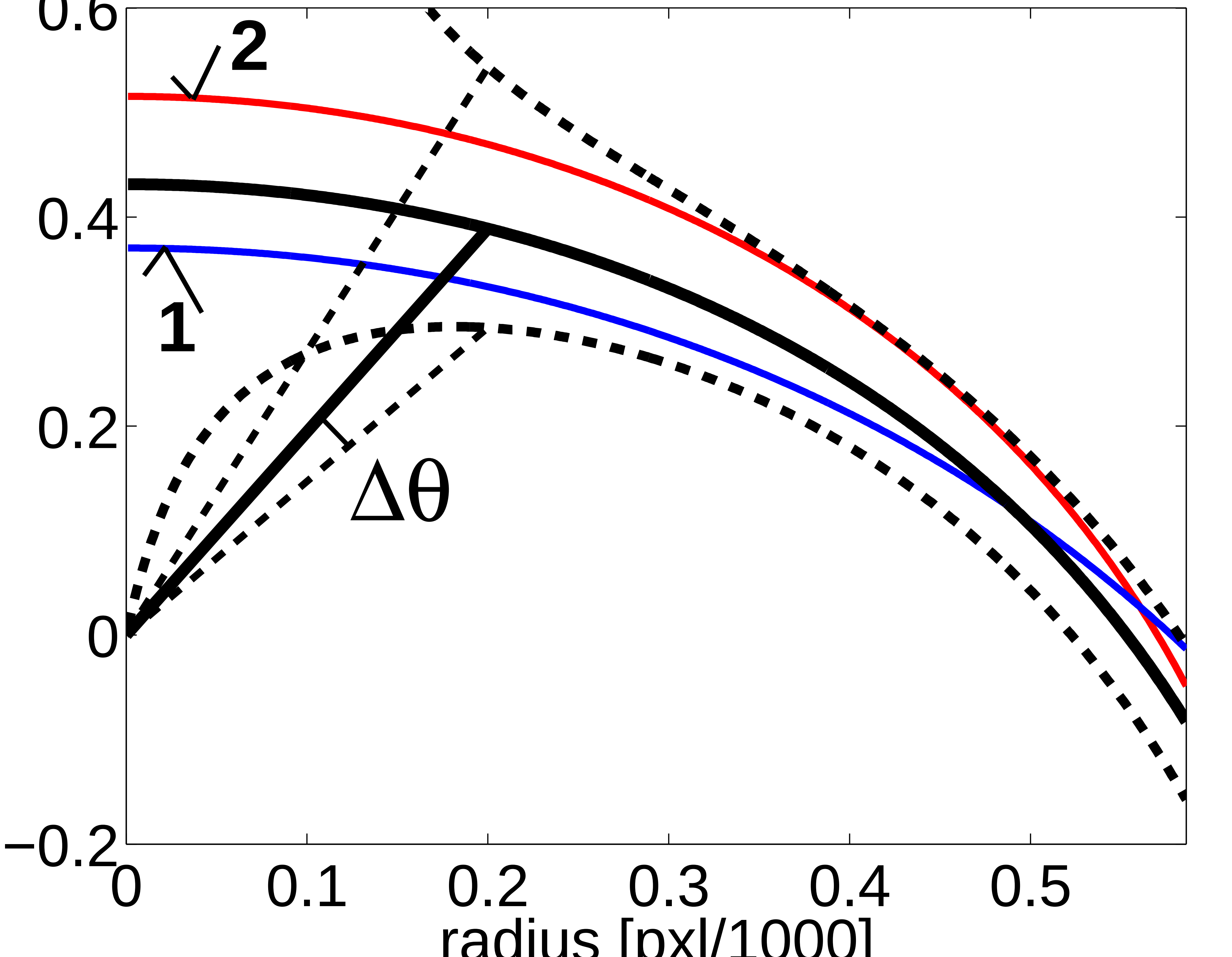

0.6
0.4
0.2
0
−0.2
f
0
0.1
0.2
0.3
0.4
0.5
radius [pxl/1000]
2
1
Δθ

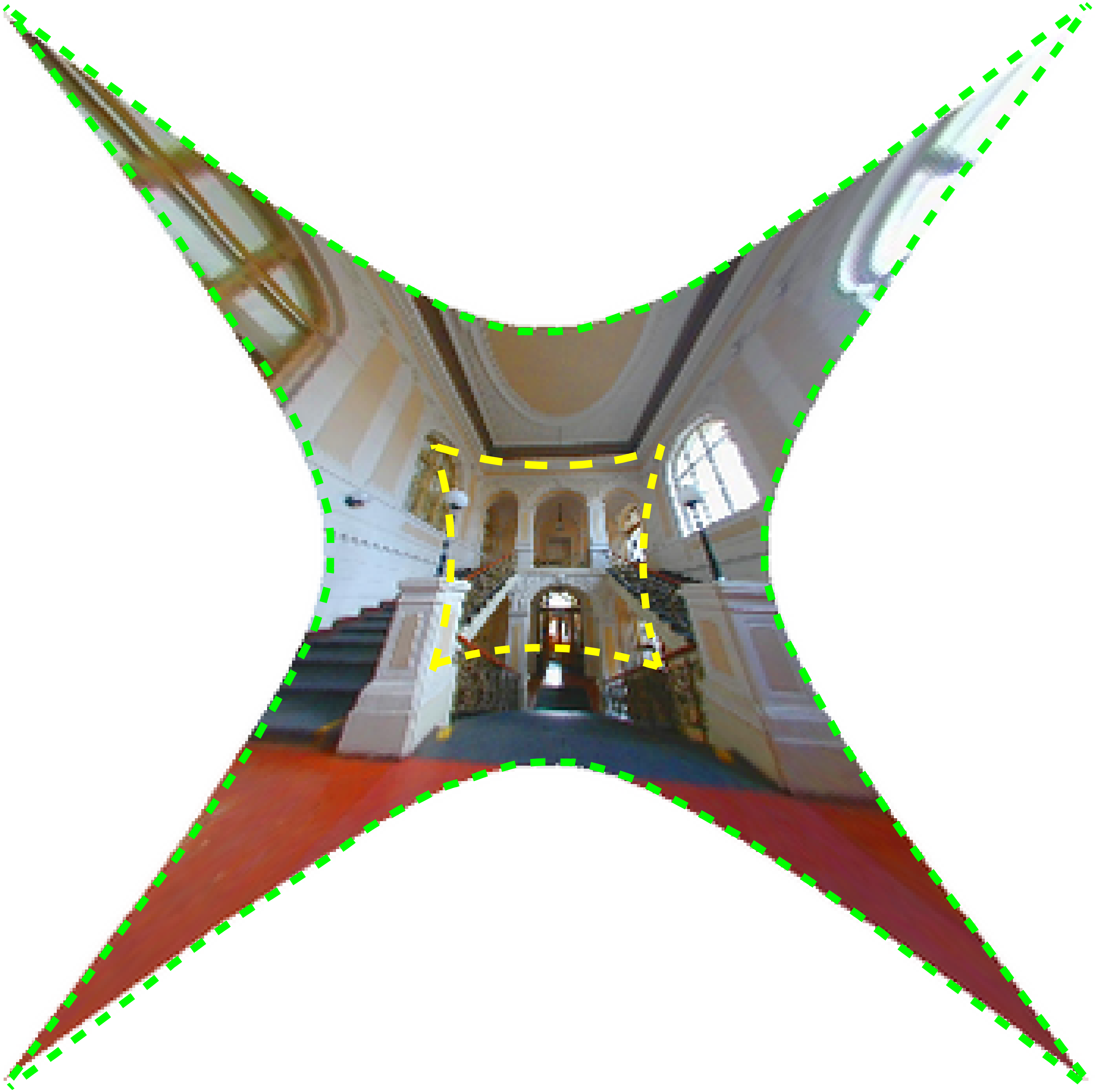

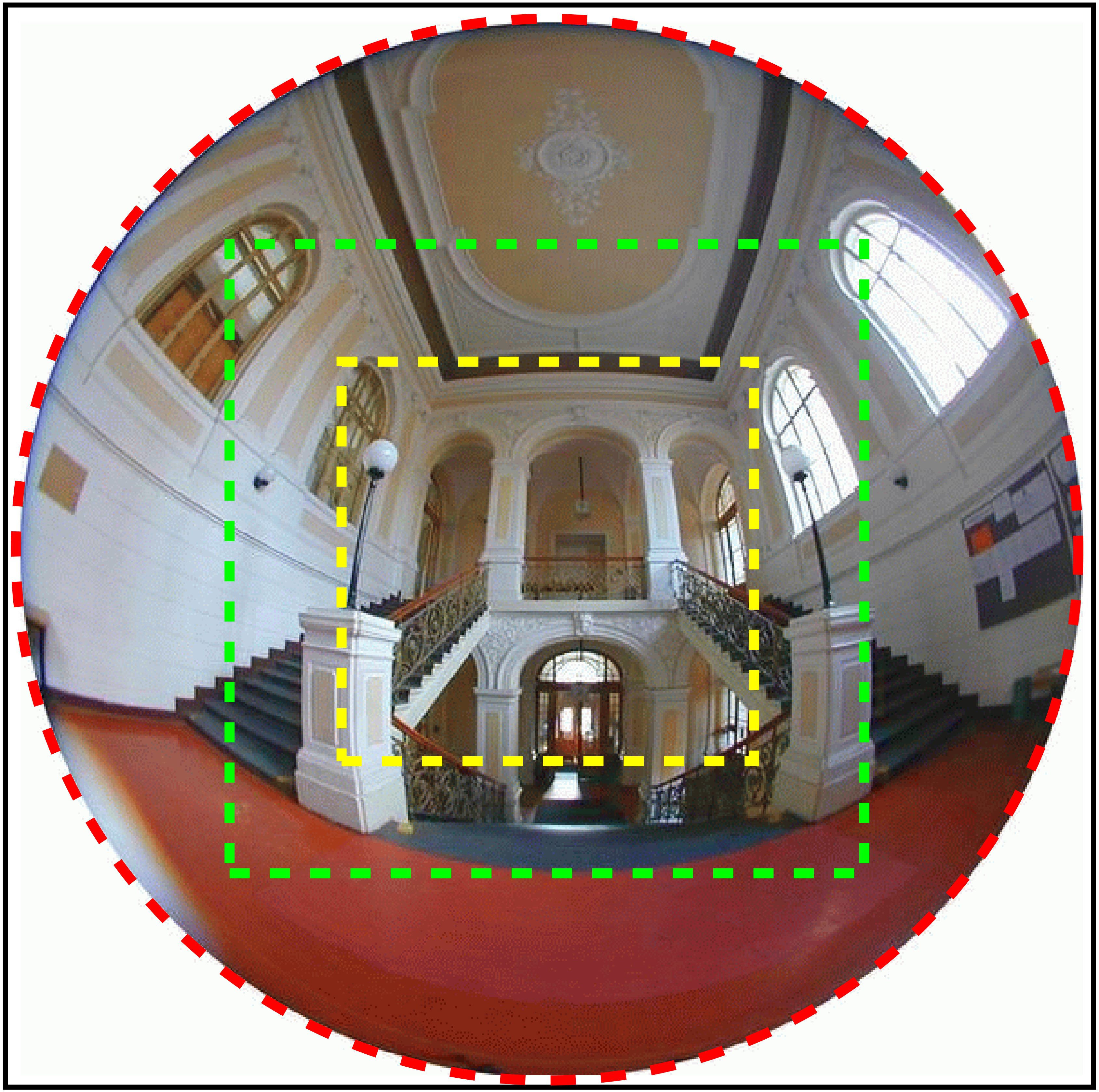

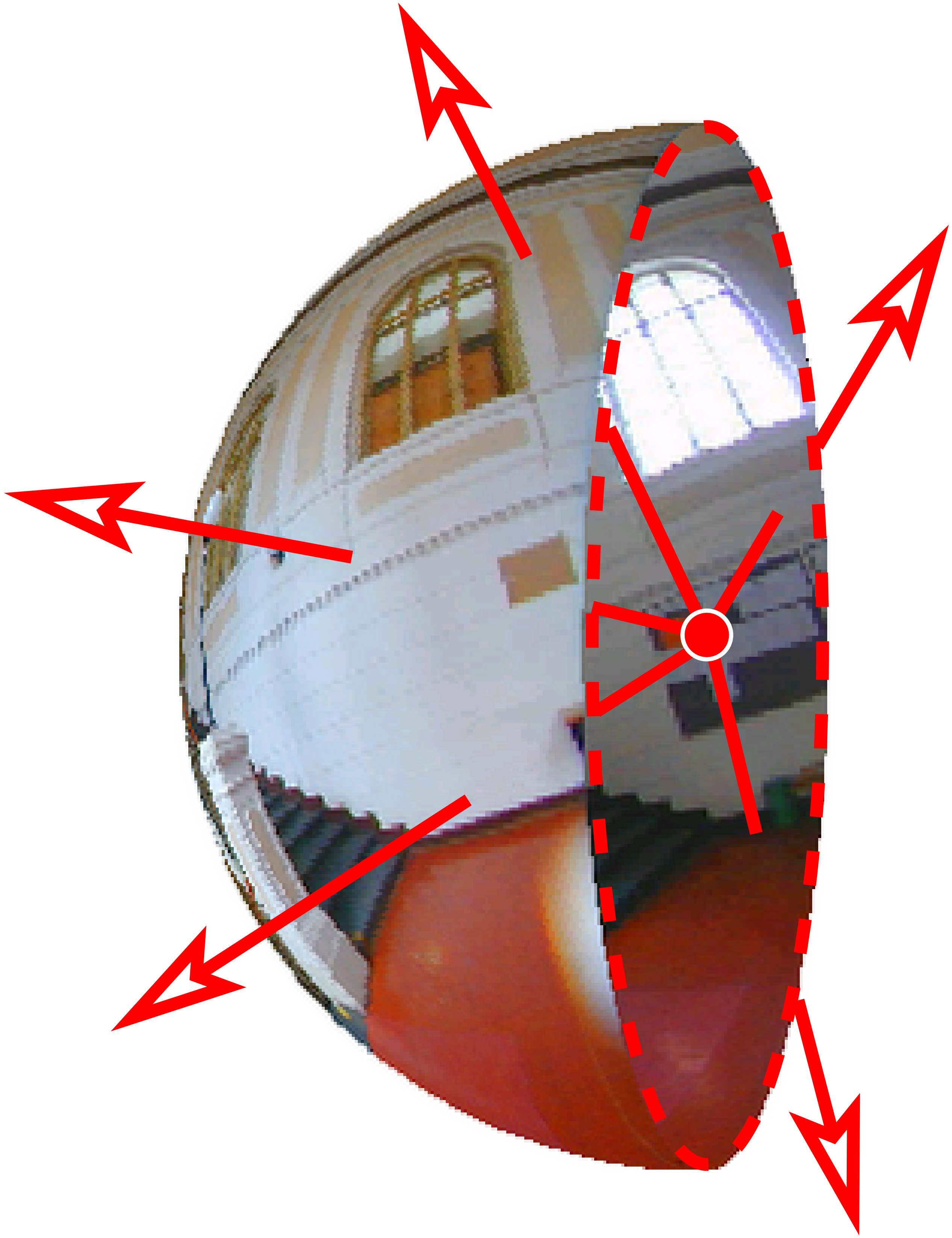

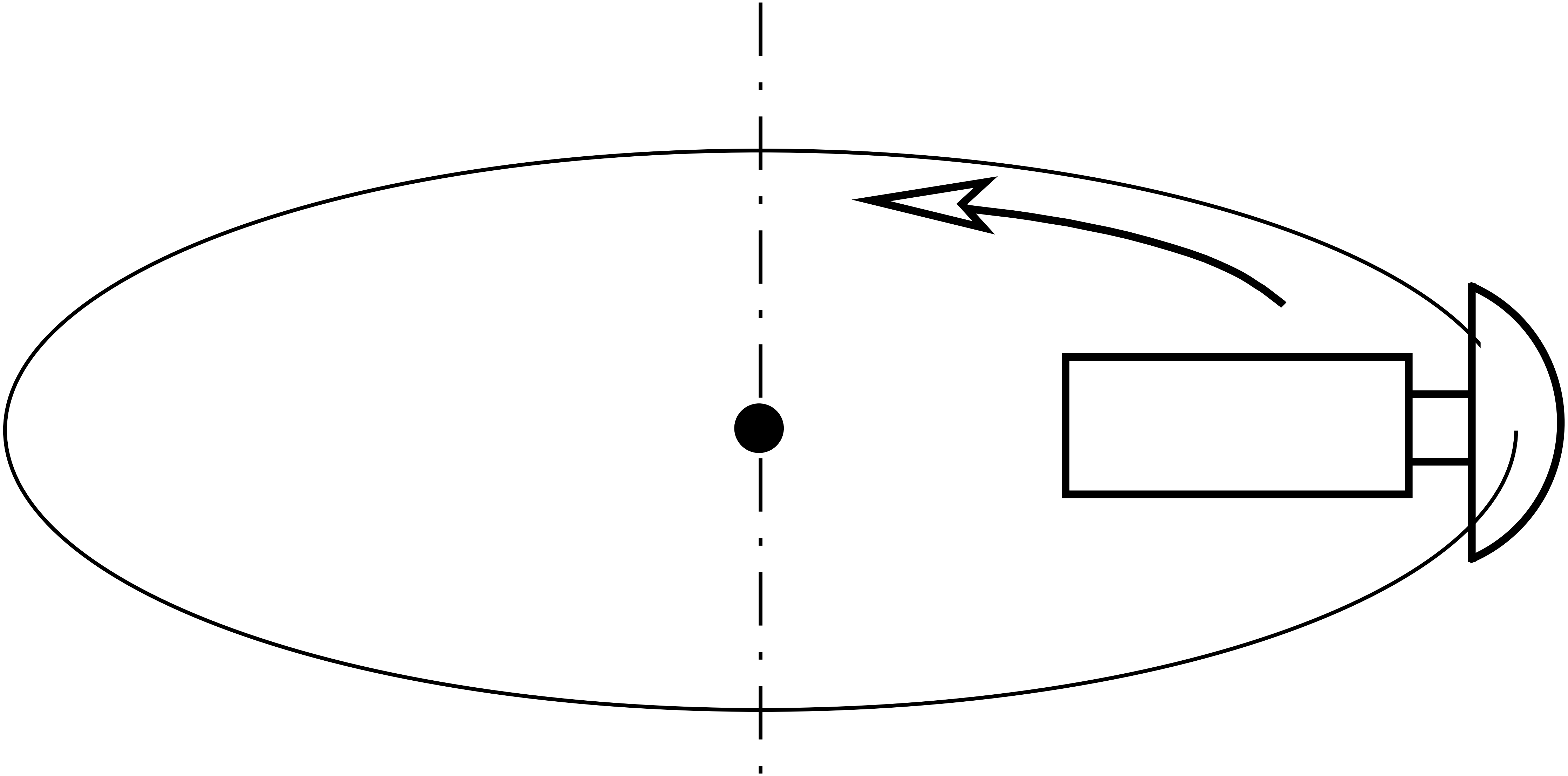

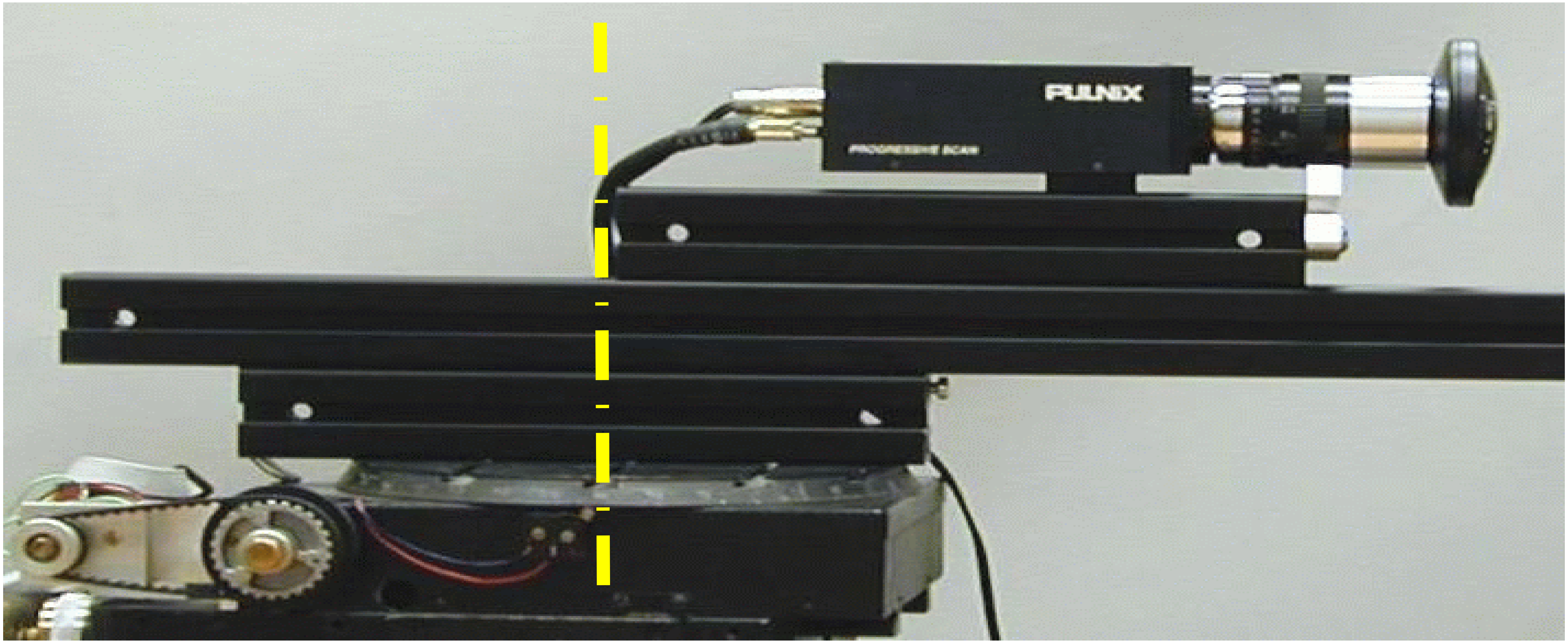
PULNIX
PROGRESSIVE SCAN

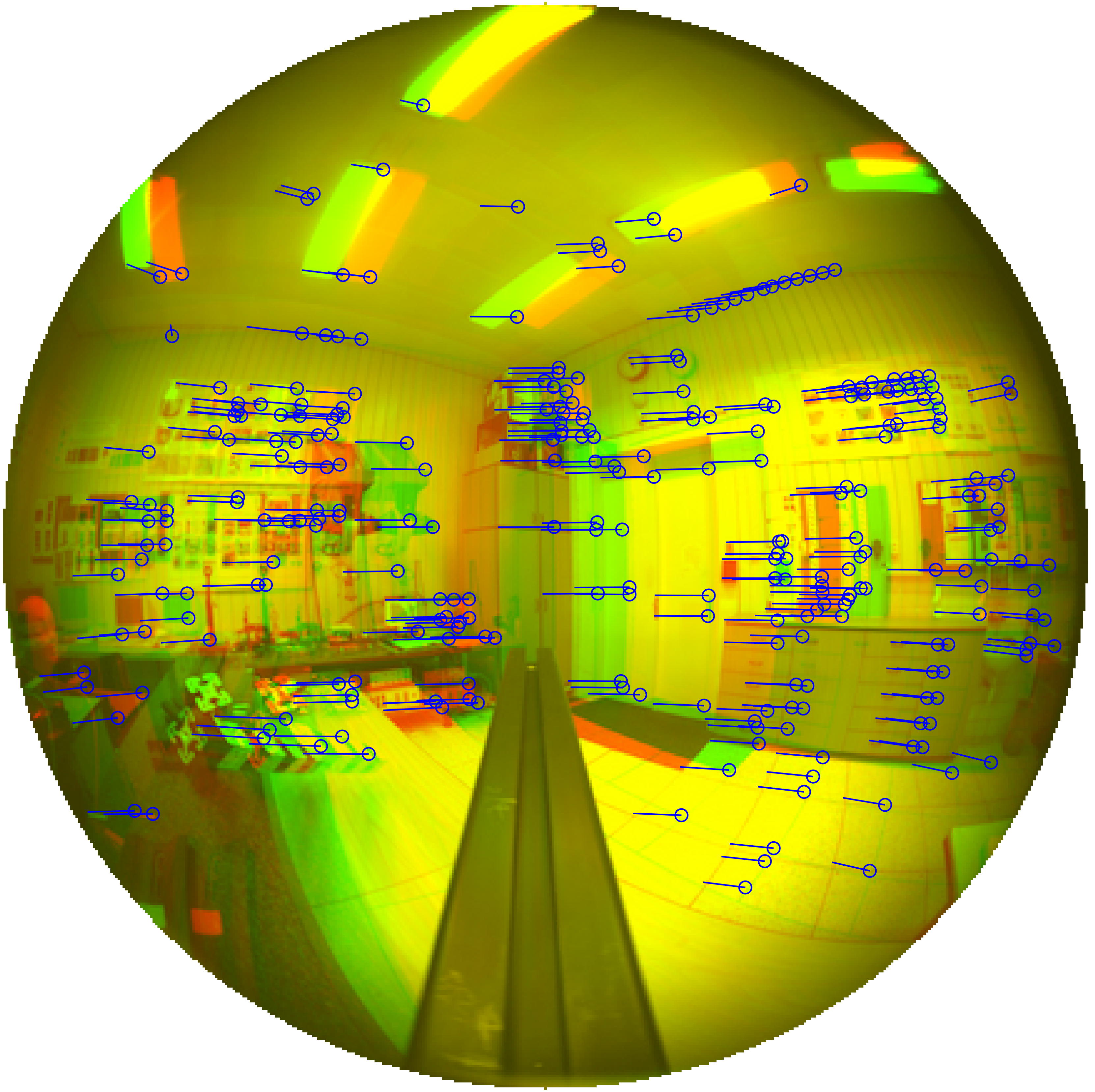

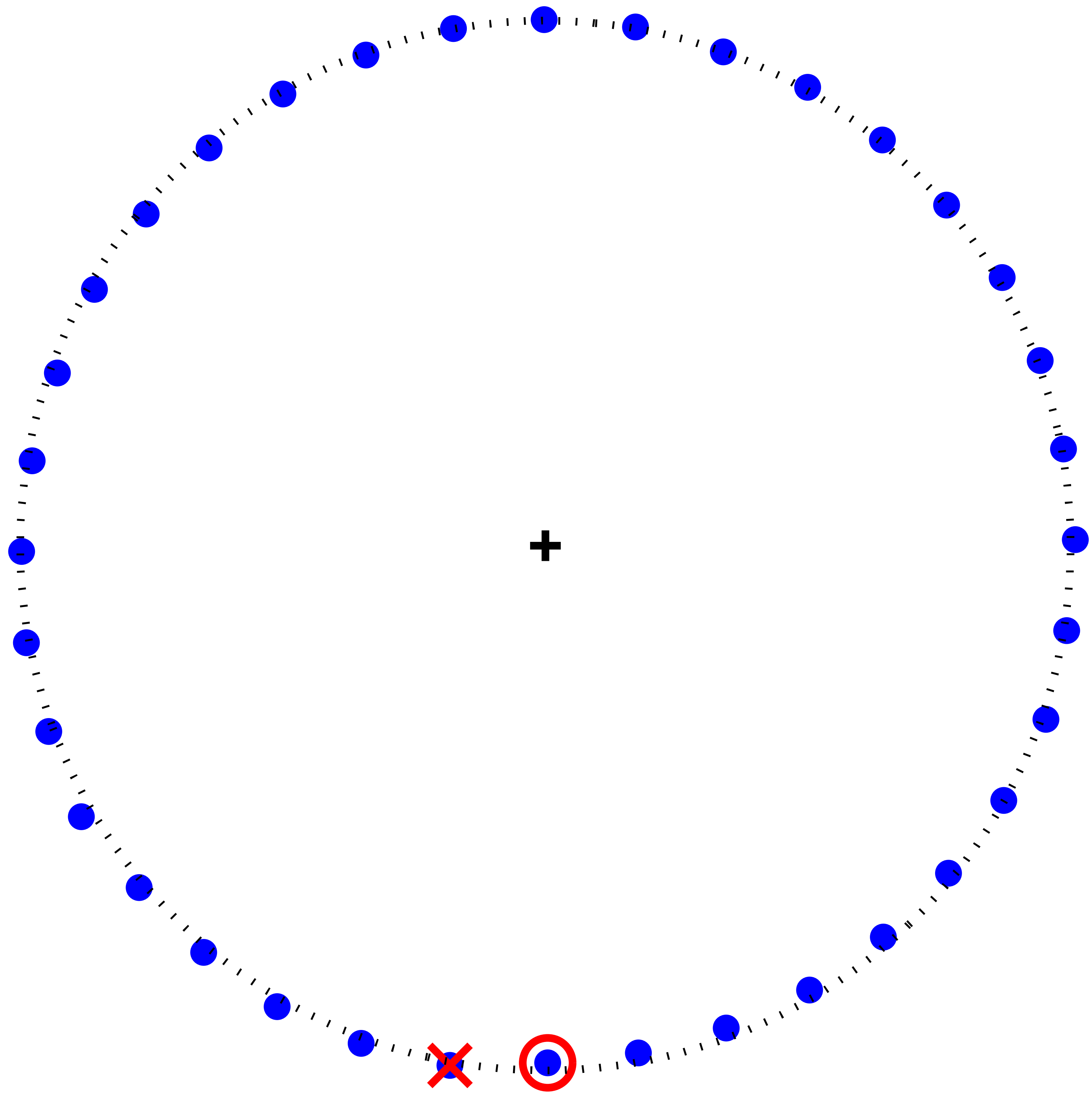

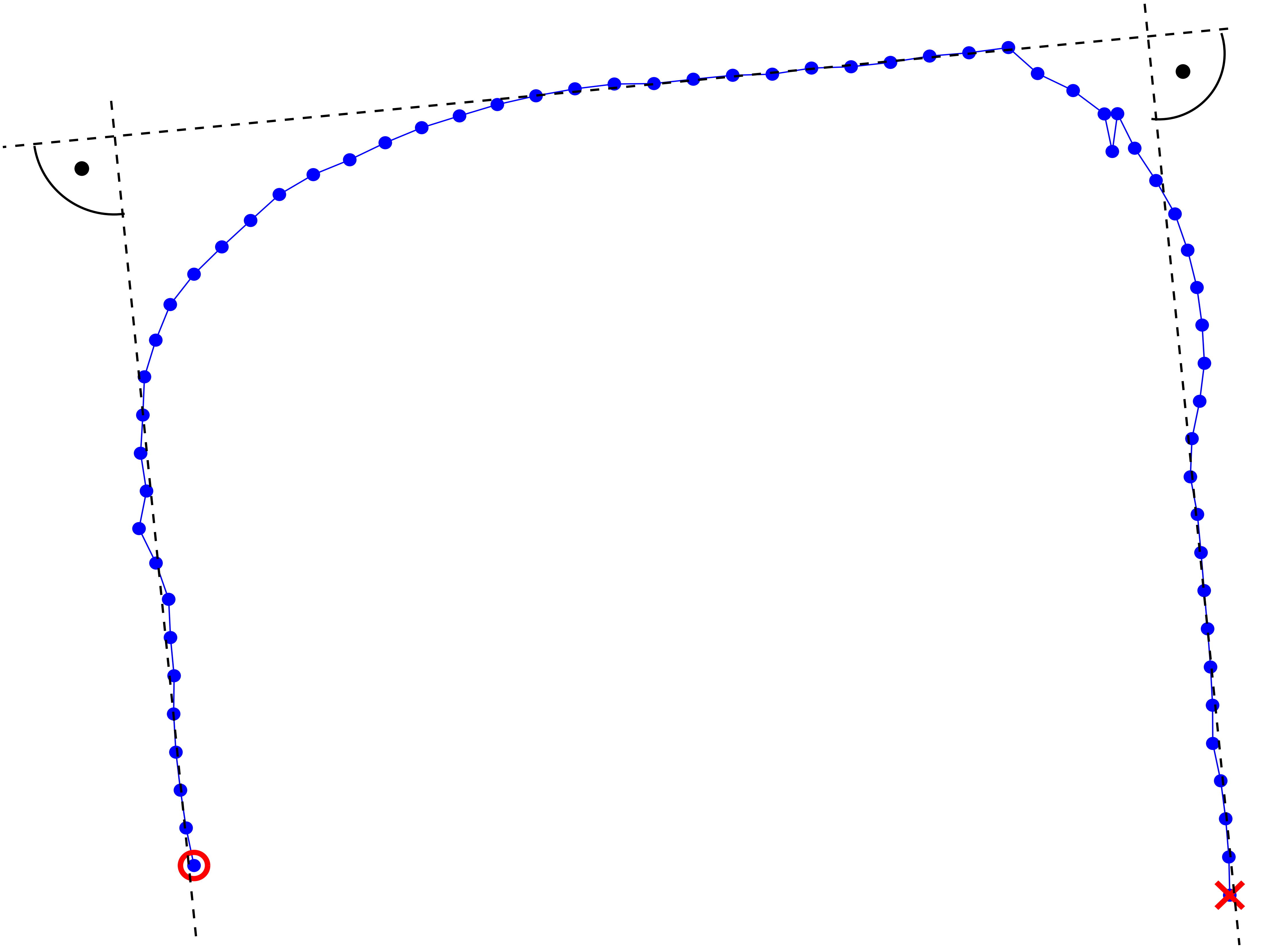

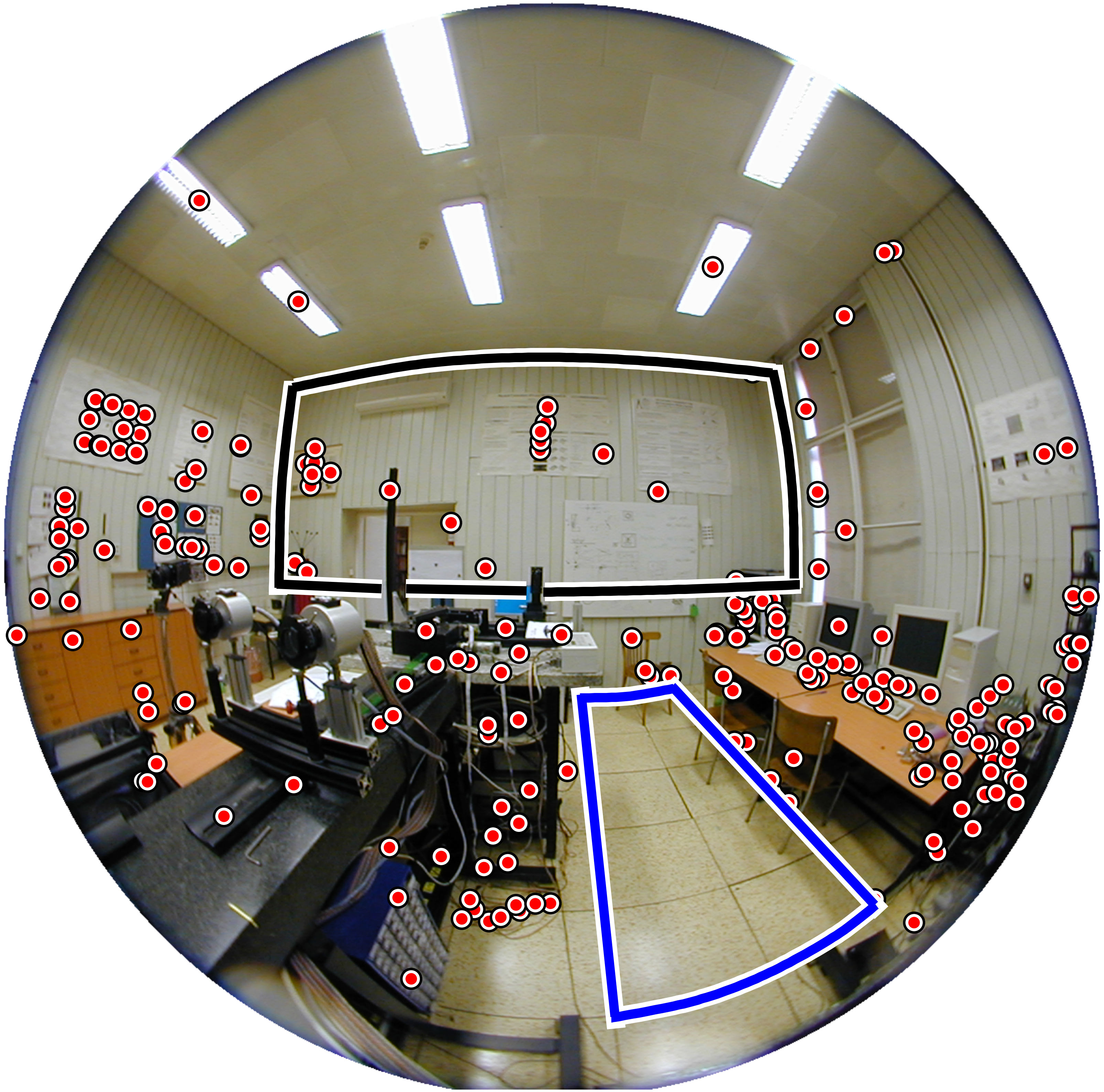

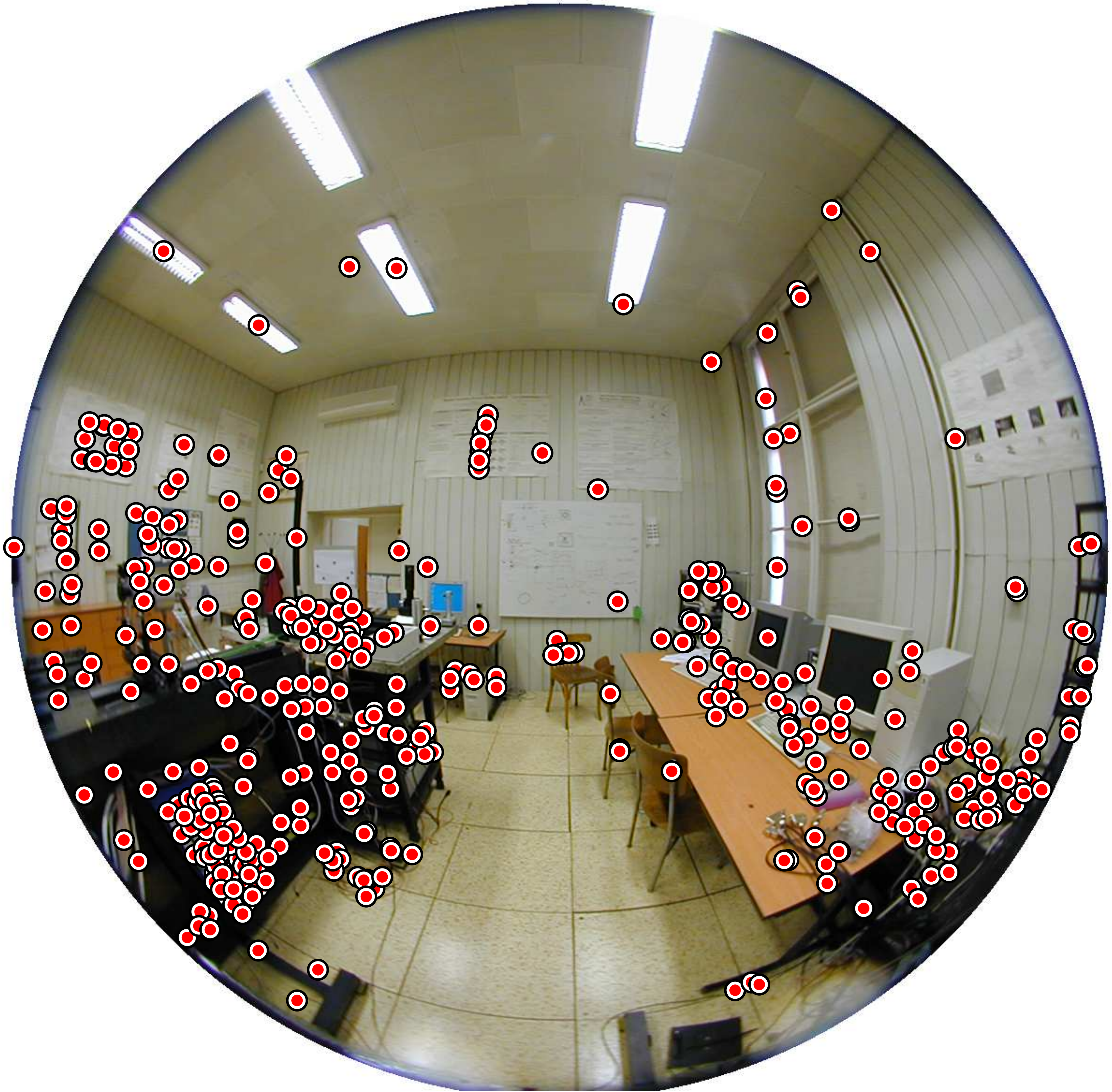

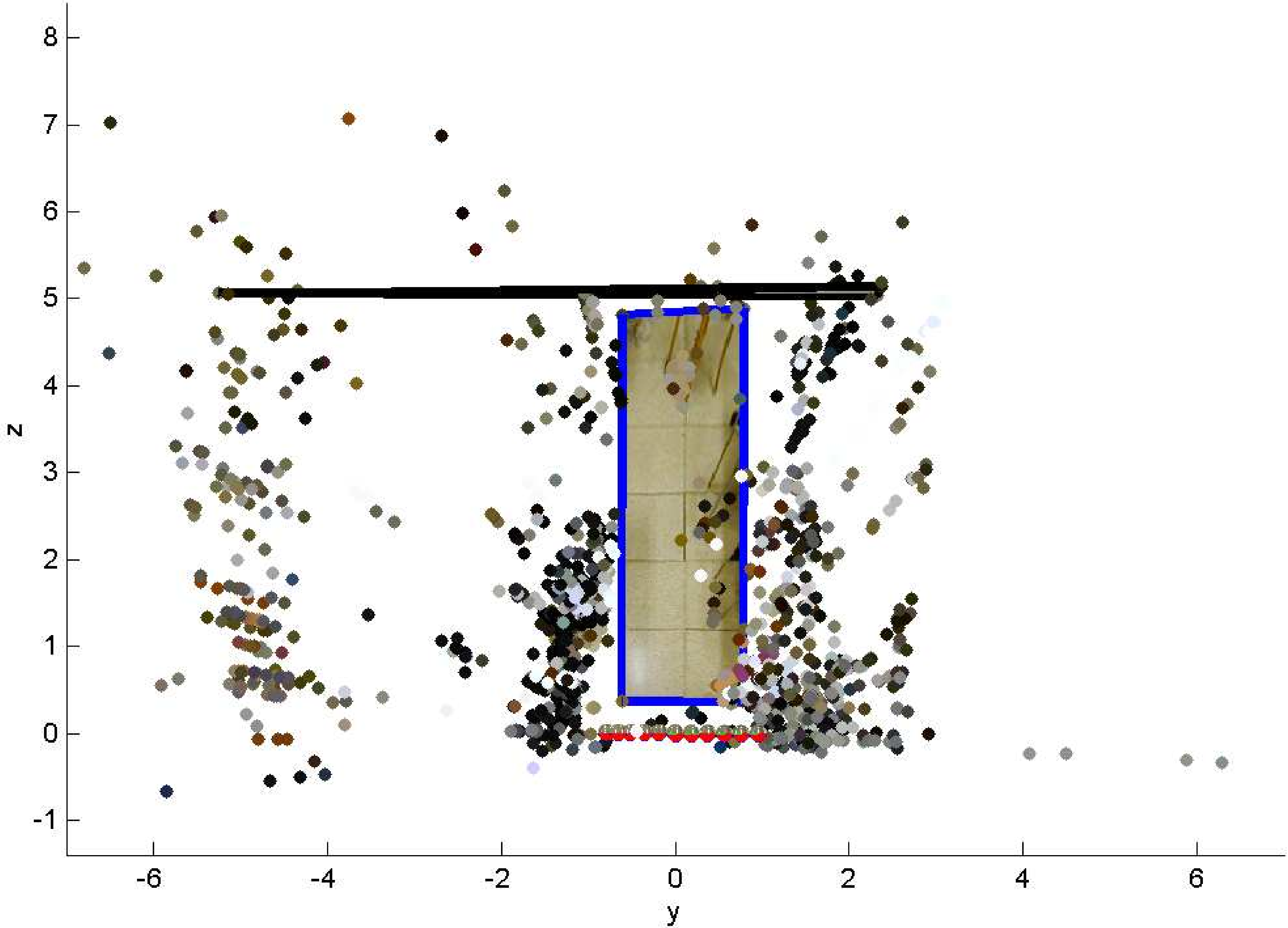
z
y
8
7
6
5
4
3
2
1
0
-1
-6
-4
-2
0
2
4
6

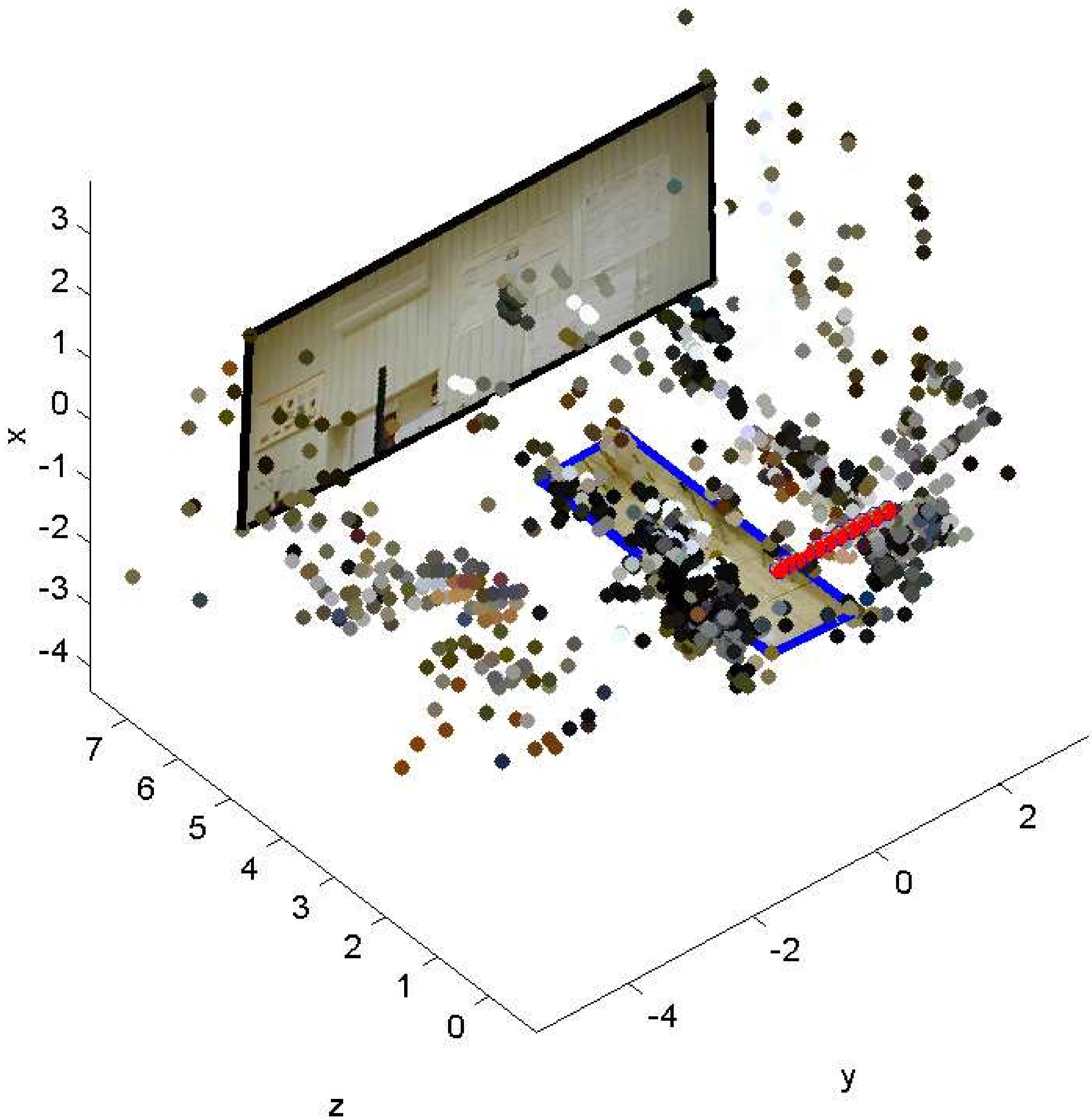

x
3
2
1
0
-1
-2
-3
-4
z
7
6
5
4
3
2
1
0
y
-4
-2
0
2

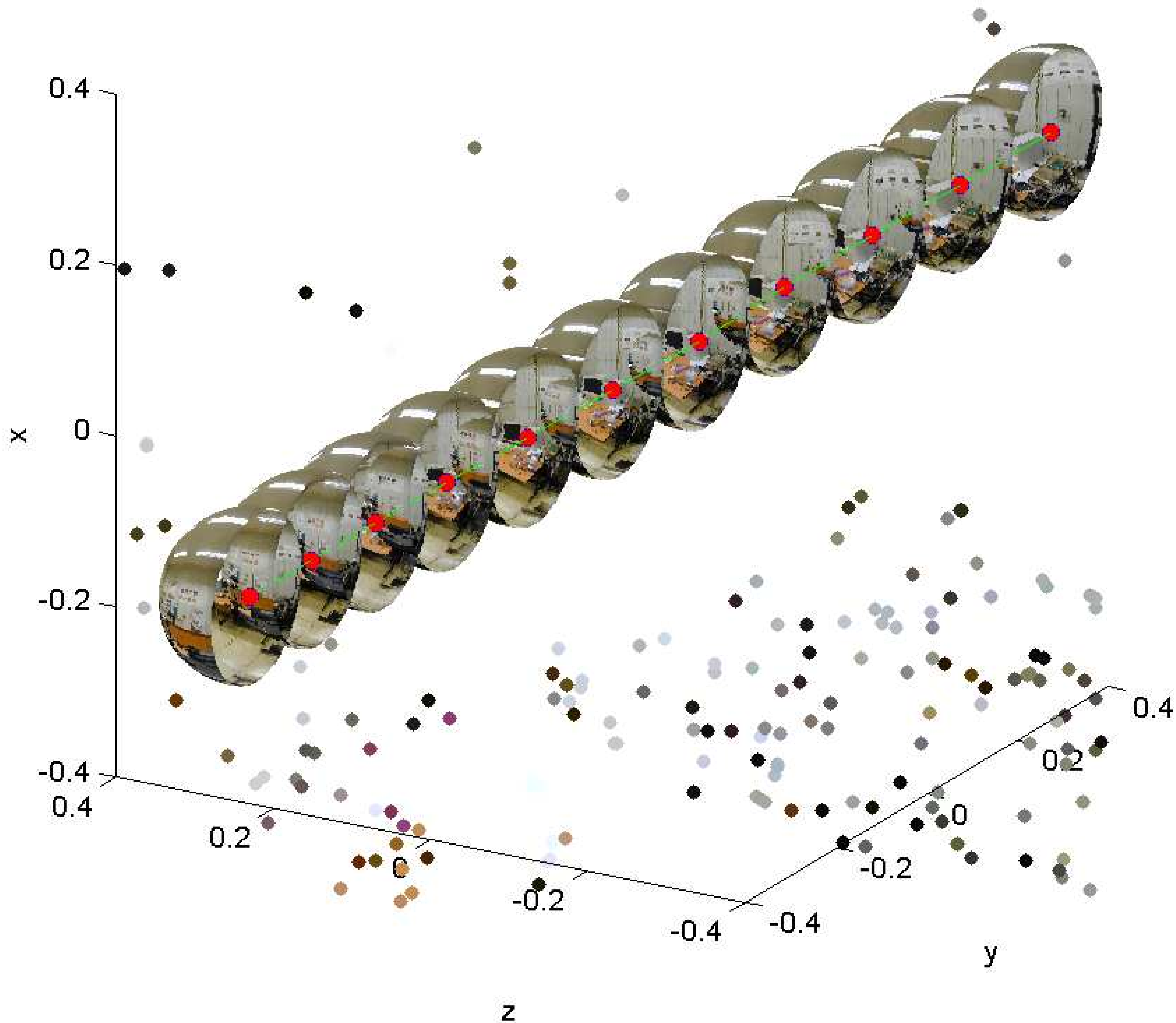
0.4
0.2
0
-0.2
-0.4
x
0.4
0.2
0
-0.2
-0.4
z
-0.4
-0.2
0
0.2
0.4
y

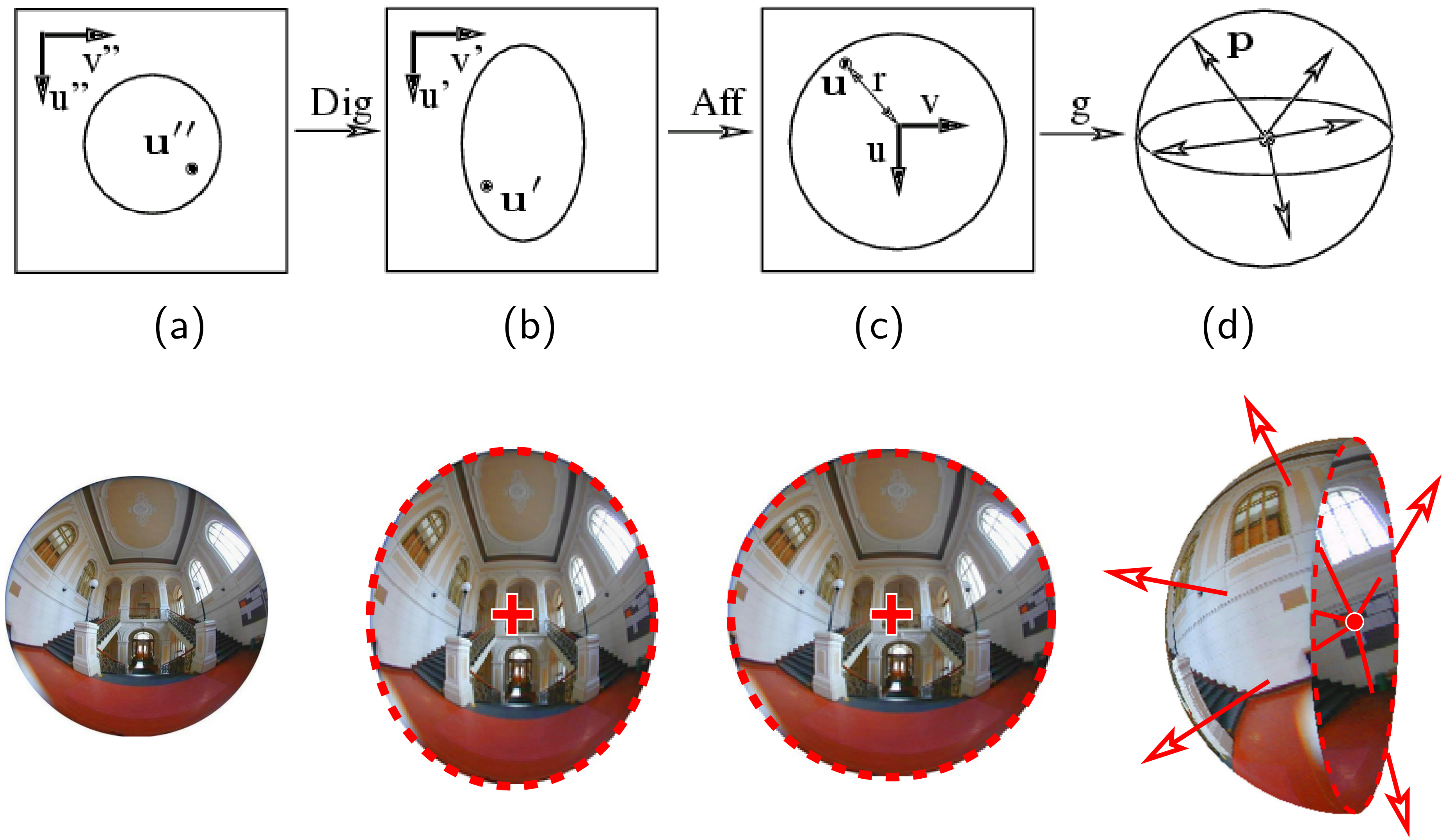

(a) – Image on the sensor plane (circular FOV)

(b) – Digitized image (non-square pixel $\rightarrow$ elliptical FOV)

(c) – Precalibrated image (ellipse $\rightarrow$ circle, radial symmetry)

(d) – Full calibration (by epipolar geometry and QEP)

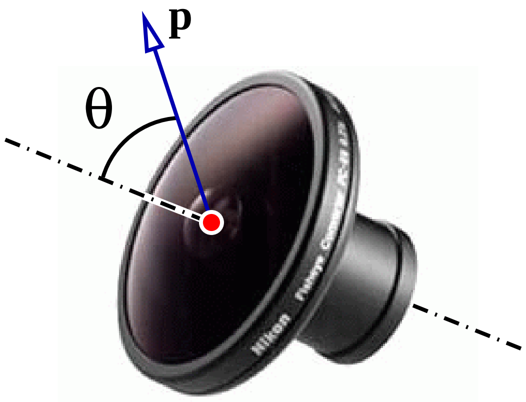

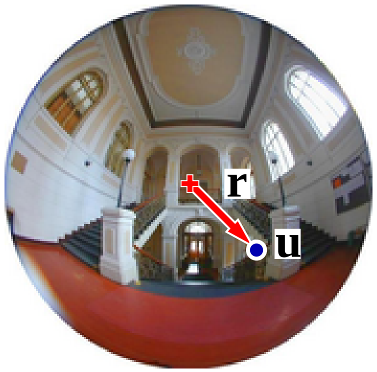

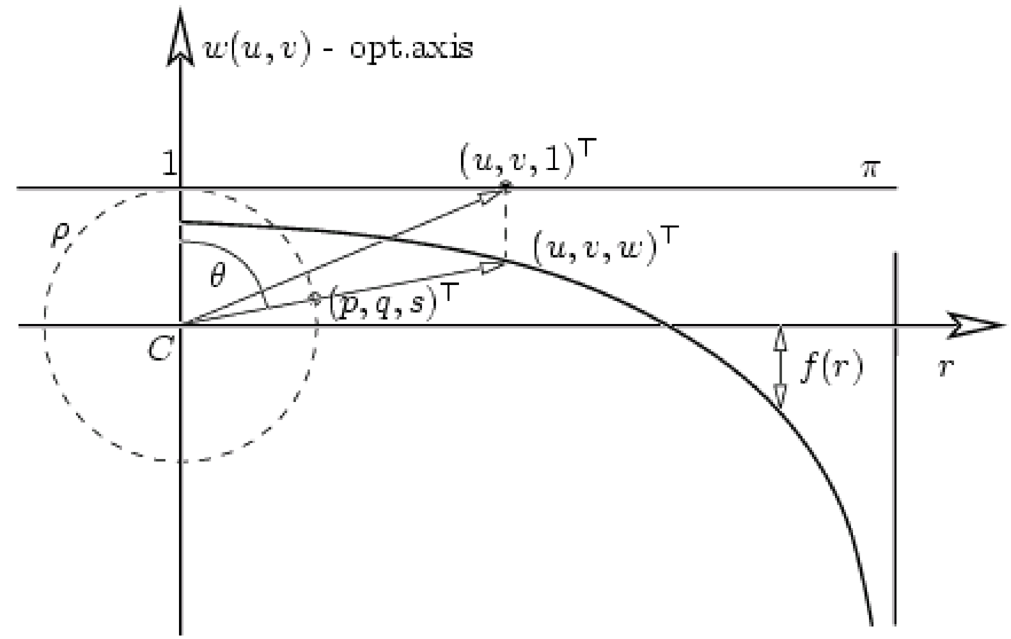

- Nonlinear camera models:

$$\boxed{\theta = \frac{ar}{1+br^2}}, \quad \boxed{r = \frac{a}{b}\sin(b\theta)}, \ldots$$

- 3D vector corresponding to an image point:

$$\mathbf{p} \simeq g(\mathbf{u}) = \begin{pmatrix} \mathbf{u} \\ w \end{pmatrix} = \begin{pmatrix} \mathbf{u} \\ f(\mathbf{u}, a, b) \end{pmatrix} = \begin{pmatrix} \mathbf{u} \\ \frac{r}{\tan\theta} \end{pmatrix} = \begin{pmatrix} \mathbf{u} \\ \frac{r}{\tan \frac{ar}{1+br^2}} \end{pmatrix}$$

Speeding up RANSAC by hierarchical fitting

- two-parametric model, 15-point RANSAC, slow for many outliers

$$\theta = \frac{ar}{1+br^2}$$

Speeding up RANSAC by hierarchical fitting

- two-parametric model, 15-point RANSAC, slow for many outliers

$$\theta = \frac{ar}{1+br^2}$$

- one-parametric model with a prior information about maximum radius R and its corresponding maximum angle of view θ_m, 9-point RANSAC, fast - most of outliers are found

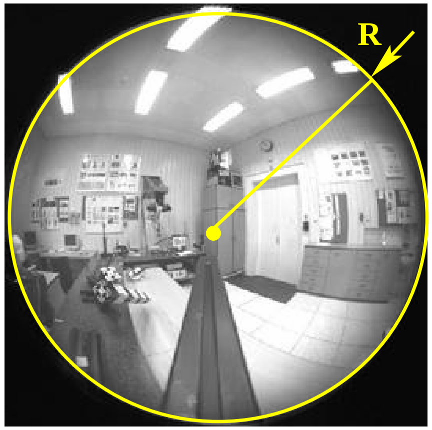

$$\theta = \frac{(1+bR^2)\theta_m}{R}\frac{r}{1+br^2}$$

Speeding up RANSAC by hierarchical fitting

- two-parametric model, 15-point RANSAC, slow for many outliers

$$\theta = \frac{ar}{1+br^2}$$

- one-parametric model with a prior information about maximum radius R and its corresponding maximum angle of view θ_m, 9-point RANSAC, fast - most of outliers are found

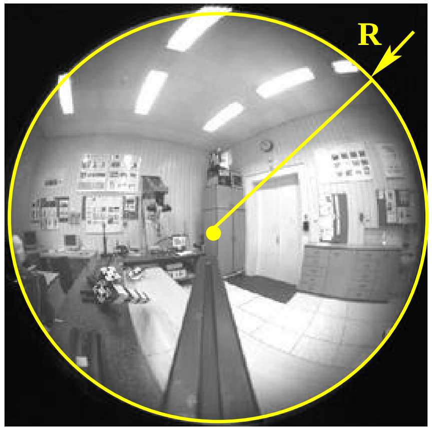

$$\theta = \frac{(1+bR^2)\theta_m}{R}\frac{r}{1+br^2}$$

- one-parametric linear model, 9-point RANSAC, fast - rough outliers are found

$$\theta = ar$$

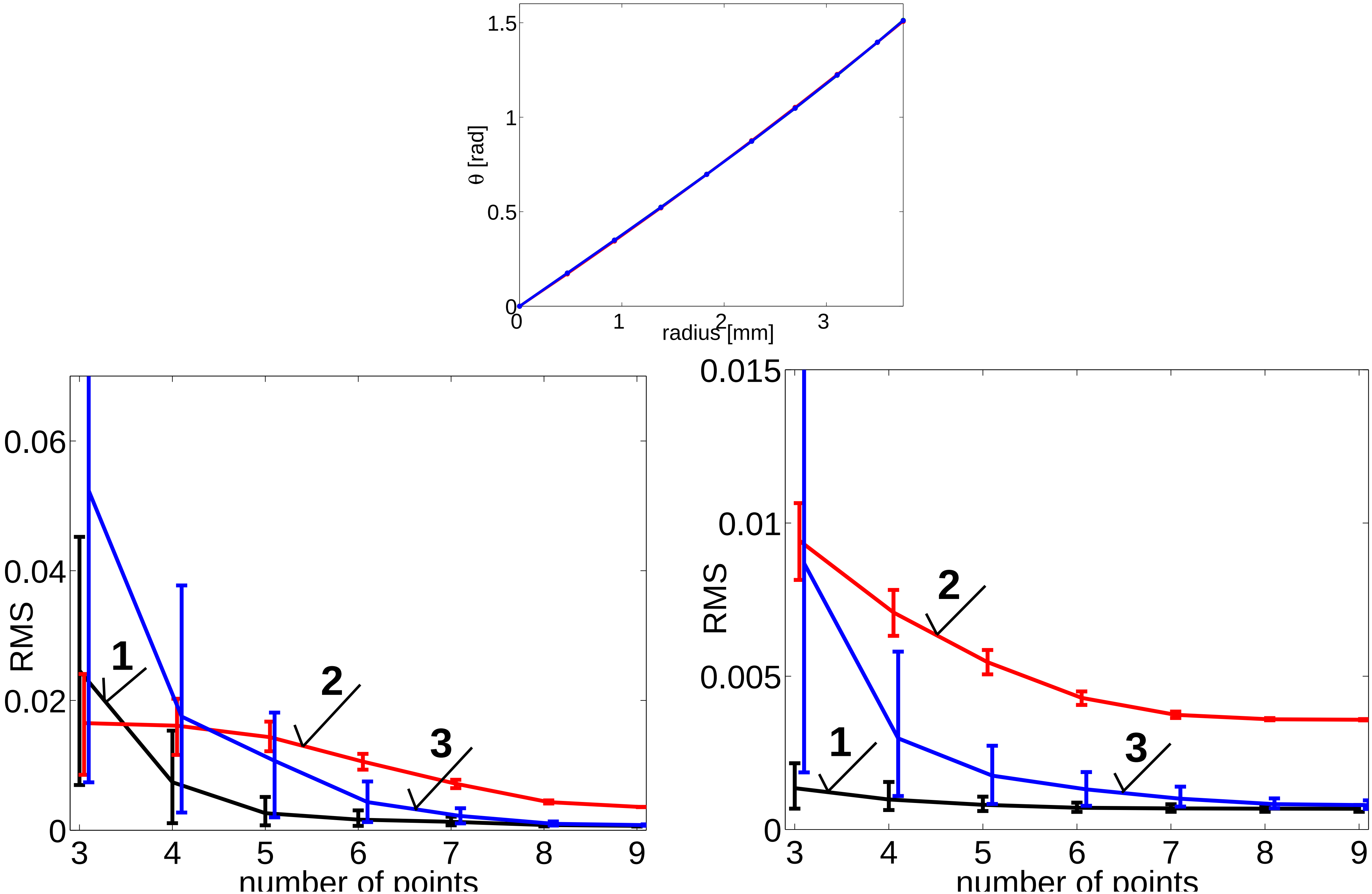

(a) (b)

1 - division model, 2 - 2^{nd} order polynomial, 3 - 3^{nd} order polynomial

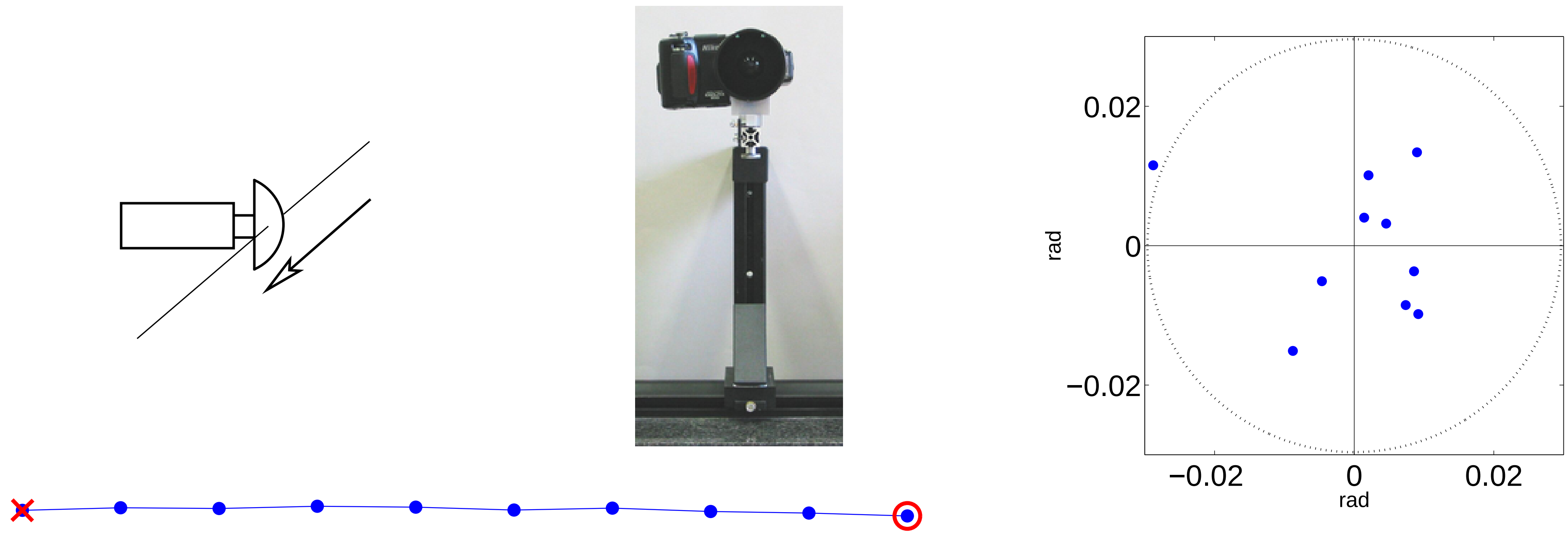

Side motion. Nikon FC–E8 lens with 1600×1200 COOLPIX digital camera.

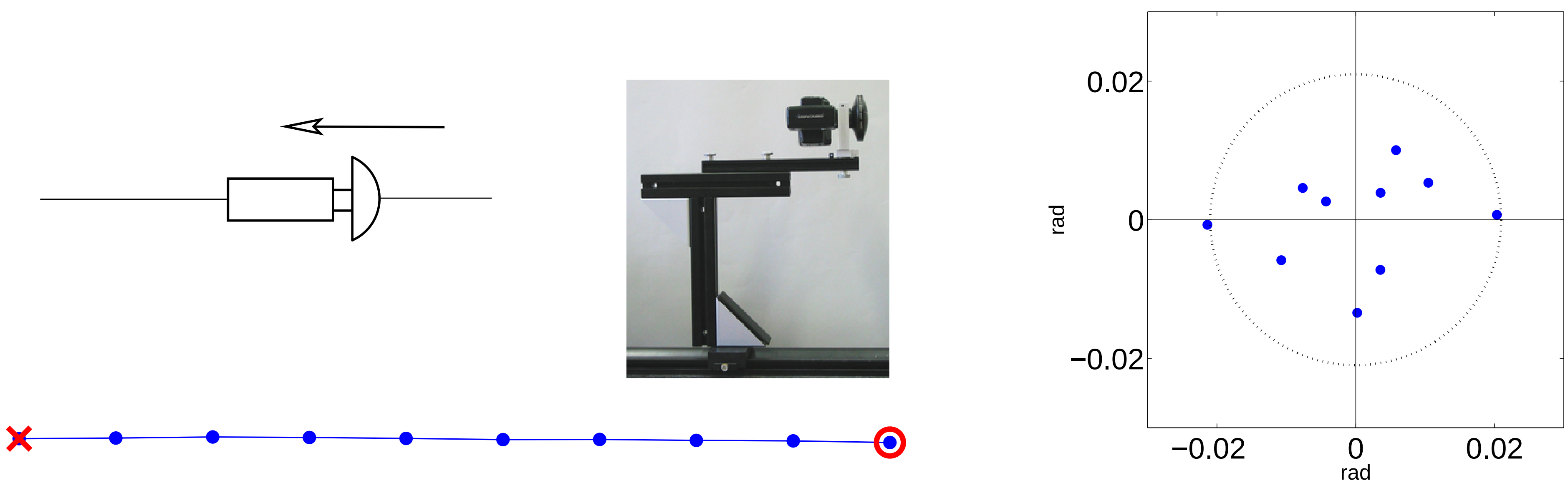

Forward motion.